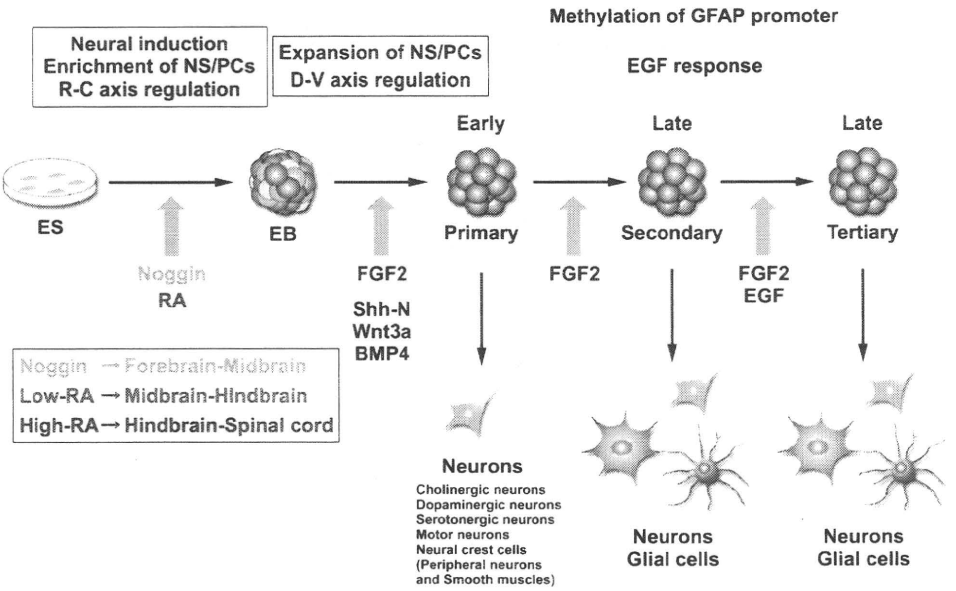

Figure 5. Schematic presentation of the spatiotemporal recapitulation of central nervous system development in ES cell-derived neurospheres in vitro. Abbreviations: BMP4, bone morphogenic protein 4; D-V, dorsoventral; EB, embryoid body; ES, embryonic stem; EGF, epidermal growth factor; FGF, fibroblast growth factor; GFAP, glial fibrillary acidic protein; NS/PCs, neural stem/progenitor cells; RA, retinoic acid; R-C, rostrocaudal; Shh-N, sonic hedgehog N-terminal peptide; Wnt, wingless.

ating 84.0 ± 3.1% $Pax6^+$ dorsal colonies with 50 ng/ml Wnt3a (Fig. 4A, 4D, 4E). The expression of *Gsh2* and *Dlx2*, which are found in the mid forebrain (supplemental online Fig. S5B), was not significantly altered by any of the treatments, and $Gsh2^+$ colonies were generated in the presence or absence of Shh-N or Wnt3a (Fig. 4A, 4D, 4E).

Similarly, in low- and high-RA neurospheres, 30–300 nM Shh-N induced ventral markers such as *Nkx6.1*, *Olig2*, and *Nkx2.2*, and 5–50 μg/ml Wnt3a upregulated the expression levels of dorsal markers, including *Pax3* and *Pax7* (Fig. 4B, 4C). Although the control low-RA neurospheres normally exhibited mainly ventral identities (Fig. 4B) and gave rise to mainly $Nkx6.1^+$ ventral colonies (82.4 ± 5.9%) and fewer with the $Pax3^+$ dorsal identity (25.7 ± 2.9%), 300 nM Shh-N increased the proportion of $Nkx6.1^+$ ventral colonies to 96.7 ± 1.5%, and 50 ng/ml Wnt3a increased the $Pax3^+$ dorsal colonies to 51.4 ± 5.8% (Fig. 4D, 4E; supplemental online Fig. S5C). Note that some colonies from low-RA neurospheres contained $HB9^+$ and $Isl\text{-}1/2^+$ ventral somatic motor neurons, regardless of the culture conditions (Fig. 4F; data not shown). In contrast, high-RA neurospheres exhibited more dorsalized characteristics (Fig. 4C). Whereas high-RA neurospheres gave rise to 44.4 ± 11.7% $Pax3^+$ dorsal colonies and a small number of $Nkx6.1^+$ ventral colonies in controls, 300 nM Shh-N induced a significant number of $Nkx6.1^+$ ventral colonies (61.2 ± 10.9%), and 50 ng/ml Wnt3a increased the $Pax3^+$ dorsal colonies (65.5 ± 9.3%) (Fig. 4D, 4E). Although Shh-N and Wnt3a could regulate the dorsoventral identities of ES cell-derived NS/PCs in all three types of neurospheres, the effects of these factors on dorsoventral identities in low-RA neurospheres was relatively small compared with those seen in noggin- or high-RA neurospheres (Fig. 4A–4E).

Finally, we examined whether Wnt3a and BMP4 directed ES cell-derived neurospheres into the neural crest lineages. Although Wnt3a increased the expression of dorsal markers, including *Pax3* and *Pax7*, it only slightly upregulated markers for neural crest lineages, *Slug* and *Snail*, in contrast to BMP4, which strongly upregulated *Slug* and *Snail* (Fig. 4B, 4C). Consistent with these results, only a small number of cells in Wnt3a-treated neurospheres appeared to be differentiated into $peripherin^+$ peripheral neurons and SMA^+ smooth muscle progenitors, as in control cultures, whereas virtually all of the cells that differentiated from BMP4-treated spheres expressed peripherin or SMA (Fig. 4G). Moreover, Wnt3a-treated neurospheres generated $Brn3a^+/peripherin^+$ sensory neurons and a small number of $Phox2b^+/peripherin^+$ autonomic neurons, whereas most of the $peripherin^+$ neurons derived from BMP4-treated low- and high-RA neurospheres were $Phox2b^+$ autonomic neurons (85.8 ± 5.0 and 89.2 ± 0.6%, respectively) and none at all were $Brn3a^+$ sensory neurons (Fig. 4H). These results were consistent with the in vivo effects of Wnt3a and BMP4 on neural crest stem cells [38]. Taken together, these results indicate that our culture system provides a variety of neural progenitors with a wide range of temporal and spatial identities, including those of the neural crest lineages (summarized in Fig. 5).

ES Cell-Derived Neurospheres Differentiated into Electrophysiologically Functional Neurons That Formed Synaptic Contacts In Vitro

To test whether the neurons generated by our in vitro system are actually functional, neurospheres were allowed to differentiate for 10–14 days without growth factors on an astrocyte feeder layer, and then the differentiated neurons were subjected to electrophysiological analysis by the whole-cell patch-clamp technique (Fig. 6). Voltage-clamp recordings of individual neurons revealed transient inward and sustained outward currents (Fig. 6C) (data not shown). From their activation voltages and time courses, we identified the transient inward current as a Na^+ current and the sustained outward current as a delayed rectifier K^+ current (Fig. 6C–6F). The transient Na^+ current was tetrodotoxin-sensitive (data not shown). The injection of a sustained positive current induced the repetitive firing of action potentials in all of the neurons tested (n = 6) (Fig. 6D). Similar results were obtained in neurons derived from low-RA neurospheres, in which a transient Na^+ current was recorded under voltage clamp in 20 of 22 neurons tested, and depolarization (single or multiple action potentials) was induced by the positive

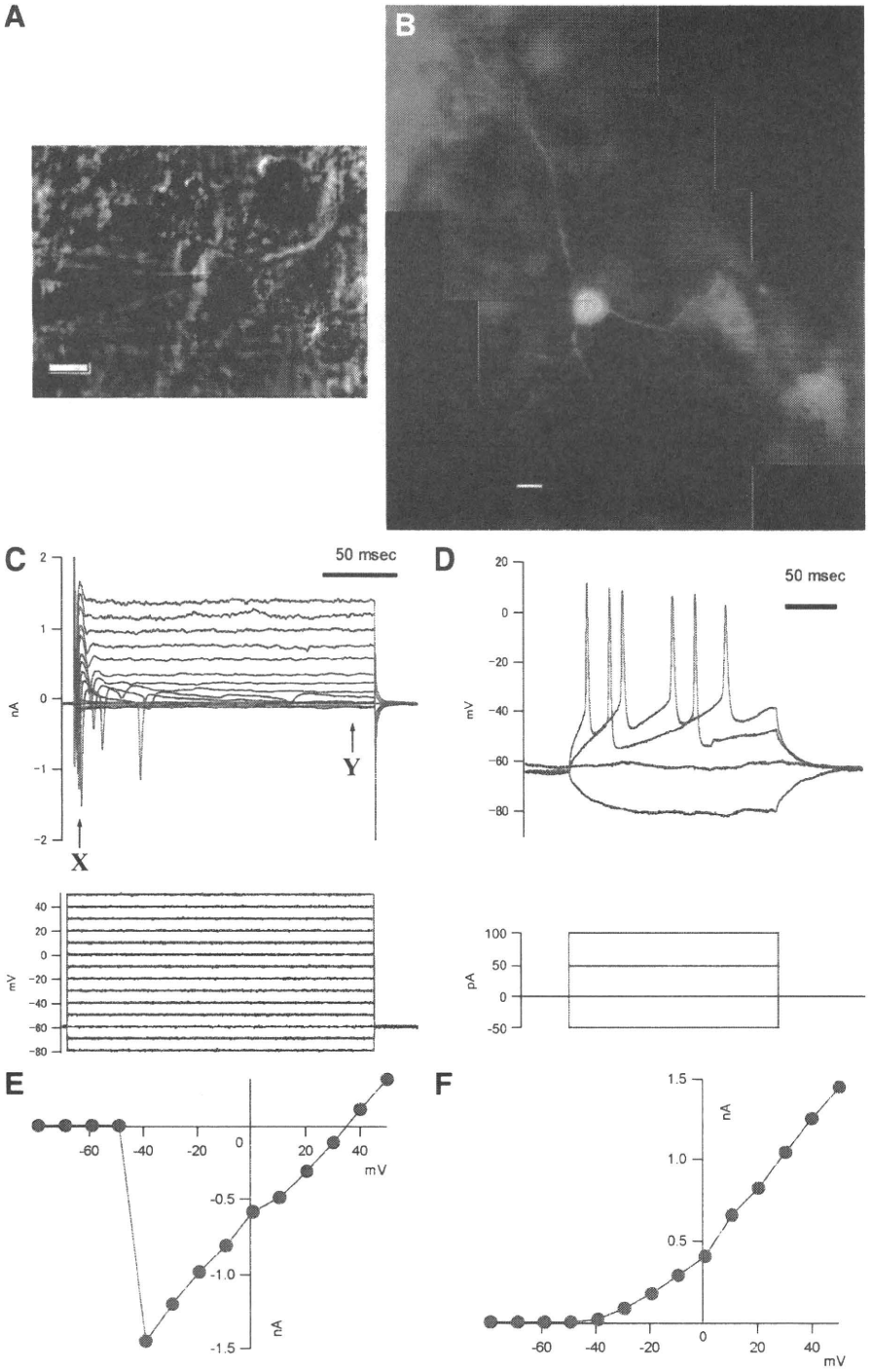

Figure 6. Electrophysiological properties of embryonic stem cell-derived neurons. Neurospheres derived from noggin-treated embryoid bodies were dissociated and differentiated on poly-L-ornithine/fibronectin-coated cover glasses, on an astrocyte feeder layer for 10–14 days, before electrophysiological analysis. **(A, B):** The cell used for the recorded data in **(C)** and **(D)** is shown in differential interference contrast and fluorescence (Lucifer yellow) micrographs. Scale bar = 10 μm. **(C):** A transient Na^+ and a sustained K^+ current were detected under voltage clamp (holding voltage, −60 mV; command voltage, from −80 to 50 mV; 10-mV step). I-V curves in panels **(E)** and **(F)** correspond to X and Y in **(C)**. X represents the transient Na^+ current and Y the sustained K^+ current. **(D):** Repetitive firing of action potentials was detected when a depolarizing current was injected under the current clamp (−50, 0, 50, and 100 pA from the bottom).

current in 3 of 4 neurons tested (data not shown). These results indicate that the ES cell-derived NS/PCs generated electrophysiologically functional neurons.

We also asked whether these neurons could form synaptic contacts in vitro. We generated an ES cell line genetically tagged to express enhanced green fluorescent protein (EGFP) under a ubiquitously expressing promoter (CAG-EGFP ES cells) and derived low-RA neurospheres from it. Because a portion of low-RA neurospheres produced $HB9^+$ somatic motor neurons (Fig. 4F), we cocultured these neurons with C2C12-derived myotubes. $EGFP^+$ ES cell-derived neurons showed neuromuscular contacts labeled by rhodamine-conjugated

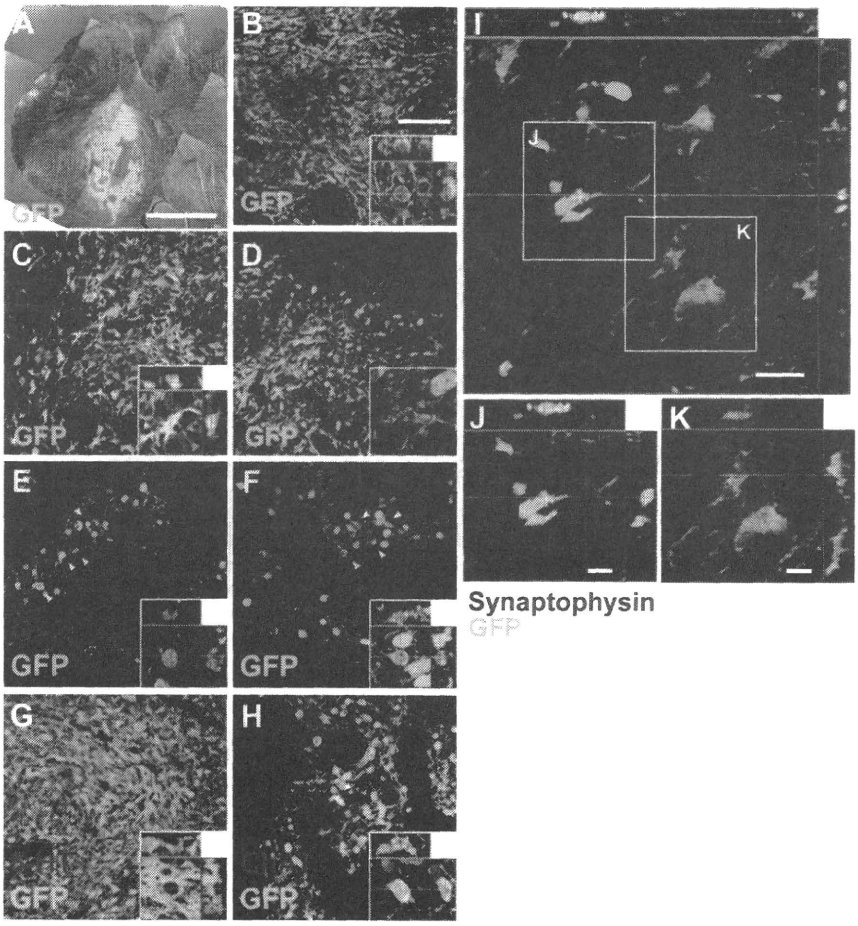

Figure 7. Low-RA neurospheres differentiated into NeuN$^+$ neurons, and when transplanted into rat lumbar spinal cord, formed synaptic contacts with the host neurons. **(A):** Low-RA neurospheres derived from CAG-enhanced GFP embryonic stem cells were transplanted stereotactically into the ventral lumbar spinal cord of Sprague-Dawley rats. Scale bar = 1 mm. **(B–H):** The rats were processed for immunohistochemical analysis 2 weeks after transplantation. Insets show higher magnifications of cells positive for both GFP and NeuN (**B**), GFAP (**C**), or subtype-specific markers (**E–H**). GFP-positive grafted cells did not differentiate into CNPase-positive oligodendrocytes (**D**). Scale bar = 100 μm for low magnification. **(I–K):** The synaptic connections of transplanted cells were studied by capturing a series of 0.5-μm optical sections with a confocal laser microscope from synaptophysin- and GFP-immunostained sections. Higher magnification images are shown in **J** and **K**. Scale bar = 20 μm (**I**), 10 μm (**J, K**). Abbreviations: ChAT, choline acetyltransferase; CNPase, 2′,3′-cyclic nucleotide 3′-phosphodiesterase; GAD, glutamic acid decarboxylase; GFAP, glial fibrillary acidic protein; GFP, green fluorescent protein; 5-HT, serotonin; NeuN, neuronal marker; TH, tyrosine hydroxylase.

α-bungarotoxin, suggesting that these neurons could form synaptic contacts in vitro (supplemental online Fig. S6).

ES Cell-Derived NS/PCs Survived and Differentiated into a Variety of Neuronal Subtypes That Formed Synaptic Connections in Rat Spinal Cord

Finally, we transplanted low-RA neurospheres derived from CAG-EGFP ES cells into the ventral lumbar spinal cord of approximately 90-day-old Sprague-Dawley rats to assess the in vivo differentiation potentials of the ES cell-derived NS/PCs. Two weeks later, the rats were sacrificed and processed for immunohistochemical analysis. The transplanted cells survived in the ventral spinal cord as cell clusters (Fig. 7A). In the treated rats, the ES cell-derived NS/PCs differentiated into NeuN$^+$ neurons and GFAP$^+$ astrocytes in some animals, but never into 2′,3′-cyclic nucleotide 3′-phosphodiesterase (CNPase)-positive oligodendrocytes (Fig. 7B; supplemental online Table 2). The neurons were mostly GAD$^+$ (GABAergic), and there were relatively few ChAT$^+$ (cholinergic), TH$^+$ (catecholaminergic), or 5-HT$^+$ (serotonergic) neurons (Fig. 7B–7F; supplemental online Table 2). Moreover, the EGFP$^+$ neurites of the transplanted neurons were extensively labeled for and surrounded by the presynaptic marker synaptophysin, indicating the formation of synaptic contacts with host neurons (Fig. 7I–7K). Similar results were obtained when low-RA neurospheres were transplanted into the lumbar spinal cord of ALS model rats harboring the mutant human *SOD1*^{G93A} gene [21, 22], although their differentiation properties in vivo varied somewhat from animal to animal (supplemental online Fig. S7; supplemental online Table 2). Thus, our ES cell-derived neurosphere culture system could be applicable to regenerative therapy for neurological disorders.

DISCUSSION

In the present study, we successfully developed an in vitro system for the efficient derivation of NS/PCs from mouse ES cells, whose temporal and spatial identities can be controlled simultaneously. By applying the neurosphere method [3], we selectively and easily cultured NS/PCs with early temporal identities and high plasticity and achieved a precise wide-range recapitulation of in vivo CNS development in vitro. This is the first report of an ES cell differentiation system that broadly and

closely mimics in vivo CNS development using a single culture protocol to generate NS/PCs.

We used noggin and RA for neural induction, which also respectively determined the rostral and caudal identities of the NS/PCs. Several lines of evidence have suggested a model in which the default positional fate of the neural plate is the rostral brain, with factors such as RA, FGFs, Wnts, and growth differentiation factors (GDFs) inducing the caudalization of neural cells in early vertebrate development [39]. One report demonstrated the effective induction of rostral neural progenitors with a combination of Dickkopf-1 and LeftyA [10]; here, we chose to use noggin instead, because BMP antagonism is essential for mammalian forebrain development [25, 26]. In our present study, noggin treatment of EBs dose dependently increased the number of neurospheres by inhibiting BMP signals in the serum-containing EB medium. Moreover, consistent with the above-mentioned model, caudalizing signal-independent noggin neurospheres adopted rostral identities. On the other hand, RA promotes the neural differentiation of ES cells concurrently with the caudalization of neural progenitors in EBs in a concentration-dependent manner in vitro: low RA produces more neural progenitors with slightly caudalized identities around the midbrain to hindbrain, and high RA induces postmitotic neurons with caudal neural tube identities rather than proliferative neural progenitors [16]. RA also causes cell cycle arrest in neuroblastoma cells by increasing the level of cyclin-dependent kinase inhibitors, such as $p27^{kip1}$, through downregulation of the ubiquitin-proteasome-dependent degradation pathway [40]. Thus, the efficient generation of neurospheres from low-RA-treated rather than high-RA-treated EBs in the present study was consistent with this concentration-dependent effect of RA on neural induction from ES cells. Moreover, we obtained neurospheres with caudal identities in an RA concentration-dependent manner by using the low-RA neurosphere protocol (forebrain, midbrain, and hindbrain) and the high-RA/short-exposure protocol (hindbrain and spinal cord). These results indicated that the rostrocaudal identity in primary neurospheres could be preserved from that acquired in the EB stage, except that the low-RA neurospheres exhibited not only midbrain-to-hindbrain but also forebrain identity. Taking into consideration the effect of RA on cell cycle arrest, these findings suggest that the rostral NS/PCs, a relatively minor population in the low-RA-treated EBs, were selectively expanded in the neurosphere condition.

In the developing CNS, distinct NS/PCs with different temporal identities are generated, depending on the developmental stage. The earliest are leukemia inhibitory factor-dependent primitive NS/PCs (E5.5–E7.5) and FGF-responsive (but not EGF-responsive) NS/PCs (E8.5–E11.5), which have the potential to generate early-born neurons; the latest are EGF-responsive NS/PCs with gliogenic potentials that cannot generate early-born neurons [1, 29–31, 41]. In addition, although ES cell-derived NS/PCs that are identical to primitive NS/PCs have been reported, these cells do not show a transition into EGF-responsive NS/PCs unless stimulated by an exogenous Notch signal [9, 41]. In contrast, our neurosphere culture system successfully enables the sequential generation of NS/PCs with early and late temporal identities just as in vivo, and it could clearly recapitulate the temporal transition of neurogenic early NS/PCs into gliogenic late NS/PCs and the acquisition of EGF responsiveness.

The gradual increase in the number of unmethylated CpGs in the GFAP promoter region, which regulates the timing of GFAP expression [20, 32, 33], from undifferentiated ES cells to secondary neurospheres, suggests that in vivo developmental changes in the epigenetic status of this region are also recapitulated to some extent in our system. Despite the remarkable augmentation of differentiation into $GFAP^+$ astrocytes from secondary neurospheres, the increase in unmethylated CpGs was not as dramatic. It is possible that cells of the neuronal lineage within the neurospheres masked this change in stem cells.

It is also noteworthy that the acquisition of gliogenic potential in the noggin neurosphere cultures was delayed compared with that in the low-RA neurosphere cultures (Fig. 2A–2C; supplemental online Fig. S1A–S1C). This is consistent with in vivo development, in which the acquisition of later identities in the caudal neural tube precedes that in the forebrain [29–31, 42, 43], indicating another advantage of our culture system, the simultaneous recapitulation of temporal and spatial specification.

We also showed that dorsoventral identity can be controlled by the administration of Shh-N, Wnt3a, and BMP4 during the neurosphere formation. The dorsoventral identity in noggin neurospheres was sharply regulated by Shh-N and Wnt3a, but the neurosphere-initiating progenitors from low- and high-RA-treated EBs seemed relatively less competent to respond to these factors. We previously showed that EBs treated with low-RA express more of the active form of Shh-N and are ventralized and those treated with high-RA express less Shh-N and acquire a dorsal identity [16]. Thus, low- and high-RA neurospheres exhibited the default identities of ventral and dorsal neural tubes, respectively. On the other hand, BMP4 had a drastic effect. BMP4 induced neurospheres that largely adopted neural crest lineages, generating $peripherin^+$ peripheral neurons and α-SMA^+ smooth muscle cells. Given that BMP2 and BMP4 promote cell death and inhibit the proliferation of rat early cortical progenitors in vitro [44], this difference between BMP4 and other factors in the magnitude of their effects on NS/PCs, including negative effects on neurosphere formation and the potential to differentiate into neural crest lineage cells, may be explained by a mechanism of selective survival. Focusing on neural crest development, because BMP2/4 and Wnt1/3a play important, concerted roles in the formation of the dorsal neural tube, including the neural crest, and are respectively involved in the generation of $Phox2b^+$ autonomic and $Brn3a^+$ sensory neurons in vivo [36, 38], the differentiation of $Phox2b^+$ autonomic and $Brn3a^+$ sensory neurons from neurospheres treated with BMP4 and Wnt3a, respectively, was consistent with the in vivo development of the peripheral nervous system (PNS), demonstrating the possible application of our culture system to the generation of neural crest lineages, including the PNS.

Another important finding of this study is that low-RA neurospheres differentiated into GAD^+, $ChAT^+$, TH^+, and $5\text{-}HT^+$ neurons both in vitro and when transplanted into the lumbar spinal cord of adult rats (Figs. 3 and 7; supplemental online Fig. 7; supplemental Table 2), indicating that these ES cell-derived NS/PCs may have maintained their in vitro-acquired identities of mainly midbrain to hindbrain even after transplantation into the more caudal in vivo environment. Interestingly, the low-RA neurospheres generated some GAD^+ GABAergic neurons (20%–40%) but relatively few $ChAT^+$ cholinergic neurons (up to 5%) in vivo (Fig. 7E, 7H; supplemental online Fig. S7G, S7J, S7K, S7N; supplemental online Table 2), even though they differentiated into many GAD^+ GABAergic and $ChAT^+$ cholinergic neurons in vitro (Fig. 3D, 3E). It is well known that neurons that make contact with their target cells and form the appropriate synaptic circuitry selectively survive better than those that do not form such connections in the nervous system [45–47]. Thus, it is reasonable to speculate that GABAergic interneurons derived from the grafted low-RA neurospheres might have been able to form synaptic contact with their target cells, which are abundant within the host spinal cord [48] and thereby survived well even in vivo. On the other hand, grafted neurosphere-derived cholinergic neurons, including motor neurons, might not have been able to

connect with their target cells, resulting in poor survival after transplantation. For example, graft-derived cholinergic motor neurons might be prevented from extending their axons out of the spinal cord by myelin-derived axonal inhibitors in the spinal cord white matter [49] and thus might have had difficulty contacting their target muscles. Alternatively, the adult spinal cord simply might not be an appropriate environment for the cholinergic differentiation of the precursor cells. Moreover, it is noteworthy that neurons derived from the transplanted NS/PCs that survived formed many synaptic contacts with the host tissues, both in wild-type and disease model animals, indicating that the ES cell-derived NS/PCs can generate functional neurons and may have the potential to regenerate functional networks in vivo, even in diseased neural tissues.

Because the complicated structure and function of the mammalian CNS develops through appropriate spatiotemporally regulated patterning, our in vitro model, which recapitulates the in vivo CNS development, may provide a simple and powerful tool for investigating the mechanisms underlying mammalian CNS development and be applicable to regenerative medicine for neurological disorders. Further studies should involve the application of a variety of factors to our culture system to mimic in vivo development, to obtain more types of neurons or neural progenitors, and to produce NS/PCs from a variety of stem cells, such as human ES cells, nuclear transfer ES cells, and induced pluripotent stem cells, which may lead to effective regenerative therapy for the damaged CNS.

ACKNOWLEDGMENTS

We are grateful to Dr. H. Niwa for the EB3 ES cells; Dr. H. Miyoshi for lentivirus vectors; Dr. O.D. Madsen, Dr. K. Campbell, Dr. J.-F. Brunet, Dr. S. Mitani, Dr. H. Kondo, Dr. P. Beachy, and Dr. Y. Takahashi for reagents; Dr. M. Yano, Dr. H. Tada, Dr. H. Kato, Dr. N. Nagoshi, Dr. W. Akamatsu, Dr. H.J. Okano, A. Tanoue, and M. Sato for technical assistance, helpful advice, and discussion; and all the members of Dr. Okano's laboratory for encouragement and kind support. This work was supported by grants from the Japan Science and Technology Agency, the Ministry of Education, Culture, Sports, Science, and Technology (MEXT), and the Ministry of Health, Labor, and Welfare (to H.O.), by a grant-in-aid for JSPS Fellows (to Y.O.), and by a grant-in-aid for the Twenty-First Century COE program from MEXT to Keio University. R.E. is currently affiliated with Department of Neurobiology, School of Medicine, Hokkaido University, Sapporo, Japan. A.K. is currently affiliated with National Institute for Physiological Sciences, Okazaki city, Aichi, Japan.

DISCLOSURE OF POTENTIAL CONFLICTS OF INTEREST

The authors indicate no potential conflicts of interest.

REFERENCES

1 Temple S. The development of neural stem cells. Nature 2001;414: 112–117.
2 Jessell TM. Neuronal specification in the spinal cord: inductive signals and transcriptional codes. Nat Rev Genet 2000;1:20–29.
3 Reynolds BA, Weiss S. Generation of neurons and astrocytes from isolated cells of the adult mammalian central nervous system. Science 1992;255:1707–1710.
4 Davis AA, Temple S. A self-renewing multipotential stem cell in embryonic rat cerebral cortex. Nature 1994;372:263–266.
5 Palmer TD, Markakis EA, Willhoite AR et al. Fibroblast growth factor-2 activates a latent neurogenic program in neural stem cells from diverse regions of the adult CNS. J Neurosci 1999;19:8487–8497.
6 Bain G, Kitchens D, Yao M et al. Embryonic stem cells express neuronal properties in vitro. Dev Biol 1995;168:342–357.
7 Lee SH, Lumelsky N, Studer L et al. Efficient generation of midbrain and hindbrain neurons from mouse embryonic stem cells. Nat Biotechnol 2000;18:675–679.
8 Kawasaki H, Mizuseki K, Nishikawa S et al. Induction of midbrain dopaminergic neurons from ES cells by stromal cell-derived inducing activity. Neuron 2000;28:31–40.
9 Tropepe V, Hitoshi S, Sirard C et al. Direct neural fate specification from embryonic stem cells: a primitive mammalian neural stem cell stage acquired through a default mechanism. Neuron 2001;30:65–78.
10 Watanabe K, Kamiya D, Nishiyama A et al. Directed differentiation of telencephalic precursors from embryonic stem cells. Nat Neurosci 2005; 8:288–296.
11 Ying QL, Stavridis M, Griffiths D et al. Conversion of embryonic stem cells into neuroectodermal precursors in adherent monoculture. Nat Biotechnol 2003;21:183–186.
12 Wichterle H, Lieberam I, Porter JA et al. Directed differentiation of embryonic stem cells into motor neurons. Cell 2002;110:385–397.
13 Su H-L, Muguruma K, Matsuo-Takasaki M et al. Generation of cerebellar neuron precursors from embryonic stem cells. Dev Biol 2006;290: 287–296.
14 Mizuseki K, Sakamoto T, Watanabe K et al. Generation of neural crest-derived peripheral neurons and floor plate cells from mouse and primate embryonic stem cells. Proc Natl Acad Sci U S A 2003;100: 5828–5833.
15 Niwa H, Masui S, Chambers I et al. Phenotypic complementation establishes requirements for specific POU domain and generic transactivation function of Oct-3/4 in embryonic stem cells. Mol Cell Biol 2002;22: 1526–1536.
16 Okada Y, Shimazaki T, Sobue G et al. Retinoic-acid-concentration-dependent acquisition of neural cell identity during in vitro differentiation of mouse embryonic stem cells. Dev Biol 2004;275:124–142.
17 Miyoshi H, Blomer U, Takahashi M et al. Development of a self-inactivating lentivirus vector. J Virol 1998;72:8150–8157.
18 Nagoshi N, Shibata S, Kubota Y et al. Ontogeny and multipotency of neural crest-derived stem cells in mouse bone marrow, dorsal root ganglia, and whisker pad. Cell Stem Cell 2008;2:392–403.
19 Yoshida S, Shimmura S, Nagoshi N et al. Isolation of multipotent neural crest-derived stem cells from the adult mouse cornea. STEM CELLS 2006;24:2714–2722.
20 Takizawa T, Nakashima K, Namihira M et al. DNA methylation is a critical cell-intrinsic determinant of astrocyte differentiation in the fetal brain. Dev Cell 2001;1:749–758.
21 Nagai M, Aoki M, Miyoshi I et al. Rats expressing human cytosolic copper-zinc superoxide dismutase transgenes with amyotrophic lateral sclerosis: associated mutations develop motor neuron disease. J Neurosci 2001;21:9246–9254.
22 Matsumoto A, Okada Y, Nakamichi M et al. Disease progression of human $SOD1^{G93A}$ transgenic ALS model rats. J Neurosci Res 2006;83: 119–133.
23 Smith WC, Harland RM. Expression cloning of noggin, a new dorsalizing factor localized to the Spemann organizer in *Xenopus* embryos. Cell 1992;70:829–840.
24 Zimmerman LB, De Jesus-Escobar JM, Harland RM. The Spemann organizer signal noggin binds and inactivates bone morphogenetic protein 4. Cell 1996;86:599–606.
25 Lamb TM, Knecht AK, Smith WC et al. Neural induction by the secreted polypeptide noggin. Science 1993;262:713–718.
26 Bachiller D, Klingensmith J, Kemp C et al. The organizer factors Chordin and Noggin are required for mouse forebrain development. Nature 2000;403:658–661.
27 Maden M. Retinoid signalling in the development of the central nervous system. Nat Rev Neurosci 2002;3:843–853.
28 Liu JP, Laufer E, Jessell TM. Assigning the positional identity of spinal motor neurons: rostrocaudal patterning of Hox-c expression by FGFs, Gdf11, and retinoids. Neuron 2001;32:997–1012.
29 Qian X, Shen Q, Goderie SK et al. Timing of CNS cell generation: a programmed sequence of neuron and glial cell production from isolated murine cortical stem cells. Neuron 2000;28:69–80.
30 Represa A, Shimazaki T, Simmonds M et al. EGF-responsive neural stem cells are a transient population in the developing mouse spinal cord. Eur J Neurosci 2001;14:452–462.
31 Tropepe V, Sibilia M, Ciruna BG et al. distinct neural stem cells proliferate in response to EGF and FGF in the developing mouse telencephalon. Dev Biol 1999;208:166–188.
32 Fan G, Martinowich K, Chin MH et al. DNA methylation controls the

timing of astrogliogenesis through regulation of JAK-STAT signaling. Development 2005;132:3345–3356.
33 Shimozaki K, Namihira M, Nakashima K et al. Stage- and site-specific DNA demethylation during neural cell development from embryonic stem cells. J Neurochem 2005;93:432–439.
34 Tanaka S, Kamachi Y, Tanouchi A et al. Interplay of SOX and POU factors in regulation of the nestin gene in neural primordial cells. Mol Cell Biol 2004;24:8834–8846.
35 Tada H, Ishii S, Kimura H et al. Identification and evaluation of high-titer anti-Sox group B antibody in limbic encephalitis. Inflamm Regen 2007;27:37–44.
36 Chizhikov VV, Millen KJ. Mechanisms of roof plate formation in the vertebrate CNS. Nat Rev Neurosci 2004;5:808–812.
37 Munoz-Sanjuan I, Brivanlou AH. Neural induction, the default model and embryonic stem cells. Nat Rev Neurosci 2002;3:271–280.
38 Kleber M, Lee H-Y, Wurdak H et al. Neural crest stem cell maintenance by combinatorial Wnt and BMP signaling. J Cell Biol 2005; 169:309–320.
39 Lumsden A, Krumlauf R. Patterning the vertebrate neuraxis. Science 1996;274:1109–1115.
40 Borriello A, Pietra VD, Criscuolo M et al. p27Kip1 accumulation is associated with retinoic-induced neuroblastoma differentiation: evidence of a decreased proteasome-dependent degradation. Oncogene 2000;19: 51–60.
41 Hitoshi S, Seaberg RM, Koscik C et al. Primitive neural stem cells from the mammalian epiblast differentiate to definitive neural stem cells under the control of Notch signaling. Genes Dev 2004;18:1806–1811.
42 Stolt CC, Lommes P, Sock E et al. The Sox9 transcription factor determines glial fate choice in the developing spinal cord. Genes Dev 2003;17:1677–1689.
43 Martens DJ, Tropepe V, van der Kooy D. Separate proliferation kinetics of fibroblast growth factor-responsive and epidermal growth factor-responsive neural stem cells within the embryonic forebrain germinal zone. J Neurosci 2000;20:1085–1095.
44 Mabie PC, Mehler MF, Kessler JA. Multiple roles of bone morphogenetic protein signaling in the regulation of cortical cell number and phenotype. J Neurosci 1999;19:7077–7088.
45 Oppenheim RW. Cell death during development of the nervous system. Annu Rev Neurosci 1991;14:453–501.
46 Buss RR, Sun W, Oppenheim RW. Adaptive roles of programmed cell death during nervous system development. Annu Rev Neurosci 2006;29: 1–35.
47 Davies AM. Regulation of neuronal survival and death by extracellular signals during development. EMBO J 2003;22:2537–2545.
48 Jankowska E. Spinal interneuronal systems: identification, multifunctional character and reconfigurations in mammals. J Physiol 2001;533: 31–40.
49 Filbin MT. Myelin-associated inhibitors of axonal regeneration in the adult mammalian CNS. Nat Rev Neurosci 2003;4:703–713.

See www.StemCells.com for supplemental material available online.

Vol 459|28 May 2009|doi:10.1038/nature08090

ARTICLES

Generation of transgenic non-human primates with germline transmission

Erika Sasaki[1], Hiroshi Suemizu[1], Akiko Shimada[1], Kisaburo Hanazawa[2], Ryo Oiwa[1], Michiko Kamioka[1], Ikuo Tomioka[1,3], Yusuke Sotomaru[5], Reiko Hirakawa[1,3], Tomoo Eto[1], Seiji Shiozawa[1,4], Takuji Maeda[1,4], Mamoru Ito[1], Ryoji Ito[1], Chika Kito[1], Chie Yagihashi[1], Kenji Kawai[1], Hiroyuki Miyoshi[6], Yoshikuni Tanioka[1], Norikazu Tamaoki[1], Sonoko Habu[7], Hideyuki Okano[4] & Tatsuji Nomura[1]

The common marmoset (*Callithrix jacchus*) is increasingly attractive for use as a non-human primate animal model in biomedical research. It has a relatively high reproduction rate for a primate, making it potentially suitable for transgenic modification. Although several attempts have been made to produce non-human transgenic primates, transgene expression in the somatic tissues of live infants has not been demonstrated by objective analyses such as polymerase chain reaction with reverse transcription or western blots. Here we show that the injection of a self-inactivating lentiviral vector in sucrose solution into marmoset embryos results in transgenic common marmosets that expressed the transgene in several organs. Notably, we achieved germline transmission of the transgene, and the transgenic offspring developed normally. The successful creation of transgenic marmosets provides a new animal model for human disease that has the great advantage of a close genetic relationship with humans. This model will be valuable to many fields of biomedical research.

The use of transgenic mice has contributed immensely to biomedical science. However, the genetic and physiological differences between primates and mice—including their neurophysiological functions, metabolic pathways, and drug sensitivities—hamper the extrapolation of results from mouse disease models to direct clinical applications in humans. Thus, the development of non-human primate models that mimic various human systems would accelerate the advance of biomedical research. In particular, genetically modified primates would be a powerful human disease model for preclinical assessment of the safety and efficacy of stem-cell or gene therapy.

The common marmoset (*Callithrix jacchus*) is a small New World primate that, because of its size, availability, and unique biological characteristics[1], has attracted considerable attention as a potentially useful biomedical research animal in fields such as neuroscience, stem cell research, drug toxicology, immunity and autoimmune diseases, and reproductive biology. Marmosets have a relatively short gestation period (about 144 days), reach sexual maturity at 12–18 months, and females have 40–80 offspring during their life. Therefore, the application of transgenic techniques to marmosets may be feasible, and would greatly facilitate the study of human disease. In contrast, the more commonly used Old World primates, such as the rhesus monkey (*Macaca mulatta*) and cynomolgus monkey (*Macaca fascicularis*), show slow sexual maturation (about 3 years) and have fewer offspring (around 10) over the female lifespan. Thus, even though marmosets are less closely related to humans than either apes or Old World primates, their potential as transgenic primate models of human disease means they may be uniquely valuable.

Obtaining large numbers of oocytes from primates for transgenic experiments is limited by ethical and economic constraints. However, because retroviral vectors allow the efficient integration of a provirus into the host genome[2–4], their use requires fewer oocytes than some other techniques. Furthermore, the injection of a lentiviral vector into the perivitelline space of a pre-implantation embryo, which is less invasive than injection into the pronucleus, is an advantageous method for generating transgenic animals. In fact, transgenic modification of rhesus monkeys using retroviral vectors and a lentiviral vector[5–7] has been attempted. In these studies, genomic integration and expression of the transgene was observed in the placenta, but not in the infants' somatic tissues, by objective analyses such as PCR with reverse transcription (RT–PCR) or western blotting.

The recombinant adeno-associated virus has been used for the targeted knockout of the cystic fibrosis transmembrane conductance receptor gene in swine fetal fibroblasts, and targeted gene knockout pigs have been generated by somatic cell nuclear transfer (SCNT) of the fibroblast nuclei into oocytes[8,9]. Although conceptually this method could be used to make targeted gene-knockout primates, marmoset SCNT techniques are not available at present.

Here we successfully produced transgenic marmosets, by injecting a lentiviral vector containing an enhanced green fluorescent protein (EGFP) transgene[10] into marmoset embryos. Four out of five transgenic marmosets expressed the EGFP transgene in neonatal tissues; the fifth expressed it in the placenta. Two showed transgene expression in the germ cells, and one fathered a healthy transgenic neonate. Our method for producing transgenic primates promises to be a powerful tool for studying the mechanisms of human diseases and developing new therapies.

Production of transgenic marmosets

In a pilot study, we showed that pre-implantation marmoset embryos obtained through natural intercourse had much better developmental potential than embryos obtained by *in vitro* fertilization (IVF). Therefore, both natural and IVF embryos were used in this study.

[1]Central Institute for Experimental Animals, 1430 Nogawa, Miyamae-ku, Kawasaki, Kanagawa 216-0001, Japan. [2]Department of Urology, Juntendo University Nerima Hospital 3-1-10 Takanodai, Nerima-ku, Tokyo 177-8521, Japan. [3]Center for Integrated Medical Research, [4]Department of Physiology, Keio University School of Medicine, 35 Shinanomachi, Shinjuku-ku, Tokyo 160-8582, Japan. [5]Natural Science Centre for Basic Research and Development, Hiroshima University 1-2-3, Kasumi, Minami-ku, Hiroshima 734-8551, Japan. [6]Subteam for Manipulation of Cell Fate, RIKEN BioResource Centre, 3-1-1 Koyadai, Tsukuba, Ibaraki 305-0074, Japan. [7]Department of Immunology, Tokai University School of Medicine, Bohseidai, Isehara, Kanagawa 259-1193, Japan.

To introduce the EGFP gene into the marmoset embryo, three kinds of self-inactivating lentiviral vectors were constructed on the basis of human immunodeficiency virus type 1 (HIV-1), and each carried a different promoter, CAG, CMV or EF1-α. The self-inactivating lentiviral vectors were named CAG-EGFP, CMV-EGFP and EF1-α-EGFP, respectively.

All lentiviral vector injections were performed at the earliest embryonic stage possible using an Eppendorf FemtoJet express and a Narishige micromanipulator. Twenty-seven IVF embryos and 64 natural embryos were injected with a high titre of the lentiviral vector, from 5.6×10^9 to 5.6×10^{11} transducing units per ml (Table 1). Because the perivitelline space of the marmoset early embryo is rather small, 16 of the 27 IVF embryos, and 49 of the 64 natural embryos, at the pronuclear-to-morula stage, were first placed in 0.25 M sucrose in PB1 medium (0.25 M sucrose medium), which made the perivitelline space expand 1.2–7.5-fold (data not shown). The lentiviral vector was then injected into the perivitelline space (Supplementary Data 1). Virus was injected into the blastocoel of the remaining 11 IVF and 15 natural embryos at the blastocyst stage, without the 0.25 M sucrose treatment (Supplementary Data 1).

Immediately after injection, 4 of the IVF and 12 of the natural embryos were transferred to recipient females. The rest were examined for the expression of EGFP, starting 48 h after injection. Among the sucrose-treated IVF and natural early embryos at 48 h after injection, 68.8% and 97.7% expressed EGFP, respectively; of the non-sucrose-treated IVF and natural embryos injected with lentivirus as blastocysts, 85.7% and 87.5% expressed EGFP, respectively (Supplementary Data 1). Therefore, 61 of the natural embryos and 19 of the IVF embryos were transferred to surrogate mothers (Table 1). For the transfers, the recipients were synchronized with the donor oocyte cycle; each recipient received 1–3 embryos per cycle, and 50 surrogate mother animals were used.

Of the surrogate mothers, seven that received natural or IVF embryos became pregnant. Three recipients miscarried on days 43, 62 and 82, and the other four delivered five healthy offspring (three singletons, one pair of twins), one male (number 666) and four females, on days 144–147 after ovulation (Fig. 1). For the infants, the lentiviral vector injection had been performed at the four-cell stage (584), the pronuclear stage (587), and the morula stage (588, 594 and 666). The EGFP transgene was driven by the CAG promoter in three newborns (584, 587 and 588) and by the CMV promoter in the other two (594 and 666; Supplementary Data 1).

Table 1 | Production rates of transgenic marmosets

	Artificial reproductive technique	Natural
Number of GV oocytes	460	No data
Number of matured oocytes (only MII)	201	No data
Number of IVFs performed (including MI)	272	No data
Number of fertilized oocytes	121	No data
Fertilization rate (fertilization per GV)	26.3%	No data
Fertilization rate (fertilization per IVF)	44.5%	No data
Lentiviral injections	27	64
EGFP expression confirmed after 48 h or later	23	52
EGFP expression	17	50
EGFP expression rate	73.9%	96.2%*
ETs	19	61
Number of surrogates	13	37
Number of pregnancies	1	6
Number of deliveries	1	3
Births	1	4
Birth rate (birth per ET)	5.20%	6.55%
Number of Tgs	1	4
Production rate (Tg per injection)	3.70%	6.25%
Production rate (Tg per ET)	5.26%	6.25%
Production rate (Tg per birth)	100	100

ET, embryo transfer; GV, germinal vesicle; MI, metaphase I; MII, metaphase II; Tg, transgenes. *$P < 0.01$, chi-squared analysis.

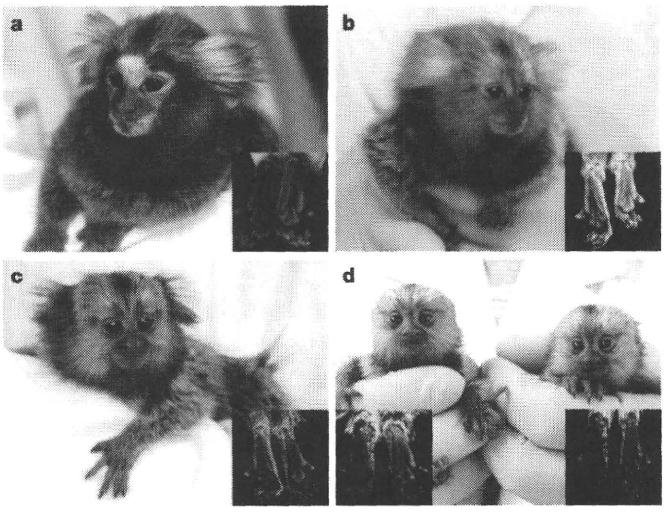

Figure 1 | Self-inactivating lentiviral vector-derived EGFP transgenic marmosets. a–d, The transgenic marmoset infants are shown. Shown are 584 (Hisui) (**a**), 587 (Wakaba) (**b**), 588 (Banko) (**c**), and twin infants 594 (Kei)/666 (Kou) (**d**). 584, 587 and 588 contained CAG-EGFP and 594/666 carried CMV-EGFP. Inset boxes in each panel show epifluorescent images of the paw of a transgenic animal (right), compared to a wild-type animal's foot pad (left). All animals except 588 expressed EGFP in their paw. 666 expressed EGFP at a slightly lower level.

EGFP transgene integration in the genome

The integration, transcription and expression of the transgene in the infant marmosets were examined using tissues that could be acquired noninvasively (placenta, hair roots, skin and peripheral blood cells). Because marmosets usually eat the placenta after delivery, only three placentae (584, 588 and that shared by twins 594/666) were collected and available for analysis[11].

The placental DNA from infants 584 and 588 showed high levels of the transgene content by real-time PCR, whereas that from 594/666 showed a relatively low level (Supplementary Data 2). The transgene was detected in the hair roots, skin and peripheral blood from infants 584, 587, 594 and 666.

Copy numbers of the integrated transgene were determined by Southern blotting analysis. At least four copies of the transgene were integrated into the genome of animal 584, and two copies were present in the genome of animal 587 (Fig. 2). Several integration sites in the genomic DNA of skin fibroblast cells, peripheral blood, the placenta of 594 and 666, and the placenta of 588 were found. Infant 588 showed transgene integration only in the placenta (Fig. 2).

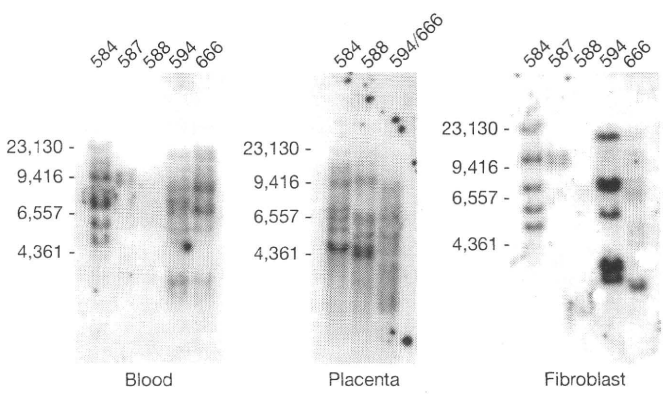

Figure 2 | Transgene insertions in several infant tissues. Southern blot analysis. All infants except 588 showed transgene integration in the skin fibroblast cells and blood, whereas 588 showed transgene integration in the placenta. The lane markers on the left of each gel represent base pairs.

To identify the chromosomal transgene integration sites, fluorescence *in situ* hybridization (FISH) was performed. Consistent with the Southern blotting analysis, the FISH results showed several integration sites in the chromosomes of peripheral blood mononuclear cells (MNCs), and further showed that each infant had different transgene integration patterns with patterns the sometimes varied among different MNCs (Supplementary Fig. 1 and Supplementary Data 3). In 584, four transgene integration sites were seen, on chromosomes 2, 7 and 13; in 587, two distinct signals were recognized in the peripheral blood lymphocyte DNA, on chromosomes 3 and 12. No signal was detected in the peripheral blood lymphocyte samples from 588, and several transgene integration patterns were seen in 594 and 666. Infant 594 had at least three different transgene integration patterns, and more than six patterns may have occurred. Infant 666 showed the largest number of integration patterns, up to 13. Moreover, although this animal was male, of the 13 investigated karyograms, eight samples were of the female karyotype, owing to haematopoietic chimaerism caused by blood exchange with his twin, 594.

Expression of the EGFP transgene

EGFP messenger RNA was detected in the hair roots of all the infants except 588 and in the peripheral blood cells of 584 and 587, by RT–PCR. Transcription of the EGFP gene was indicated in all of the placental samples, 584, 588 and 594/666 (Fig. 3a–c).

To assess EGFP expression in tissues, EGFP fluorescence was examined directly by fluorescence microscopy, and immunohistochemical analysis of the hair roots, frozen sections of a small piece of ear tissue, and placenta samples was performed (Fig. 3d–g). EGFP was strongly expressed in the epidermal cells of the ear tissue and stromal cells of the placenta. In all of the animals except 588, EGFP expression was observed in the hair roots and skin. Placental samples from 584 and 588 also showed high levels of EGFP, but it was undetectable in 594/666 (Supplementary Figs 2–4).

Peripheral blood samples were subjected to flow cytometric analysis using a FACScant. FACS analysis showed EGFP-positive peripheral blood MNCs in 584 and 587. The proportion of EGFP-positive cells was 15.7 and 19.1%, respectively (Fig. 3h). The flow cytometry results corresponded well with those from RT–PCR. Among the peripheral blood cells, the EGFP-positive percentage of granulocytes, lymphocytes and monocytes was 34.5, 3.3 and 18.0% in 584, and 47.7, 4.6 and 20.0% in 587, respectively (Supplementary Fig. 5).

Germline transmission of the transgene

At the moment when two of the animals (666 and 584) became sexually mature, the transgene expression in their gametes was analysed. Semen samples were collected from 666, and live spermatozoa were obtained by the swim-up method in TYH medium. RT–PCR analysis demonstrated the presence and expression of the transgene in the germ cells of 666 (Fig. 4a). IVFs were then performed using semen collected from 666 and wild-type oocytes to analyse the fertility of the germ cells carrying the transgene. Fluorescence microscopy showed that 20–25% of the IVF embryos strongly expressed EGFP, as shown in Fig. 4b. Furthermore, three pre-implantation live natural embryos were collected from female animal 584, and one of these embryos strongly expressed EGFP. The IVF embryos from 666 and two of the natural blastocyst embryos from 584 were shown to express the EGFP transgene by RT–PCR (Fig. 4a). Three EGFP-positive IVF embryos from the male animal (666) were then transferred into a surrogate mother. One neonate (687) was delivered at full term by caesarean section, and this neonate carried the EGFP gene and expressed the transgene in skin (Fig. 4c–e), but not in the placenta and hair.

Discussion

To our knowledge, this is the first report of transgenic non-human primates showing not only the transgene expression in somatic tissues, but also germline transmission of the transgene with the full, normal

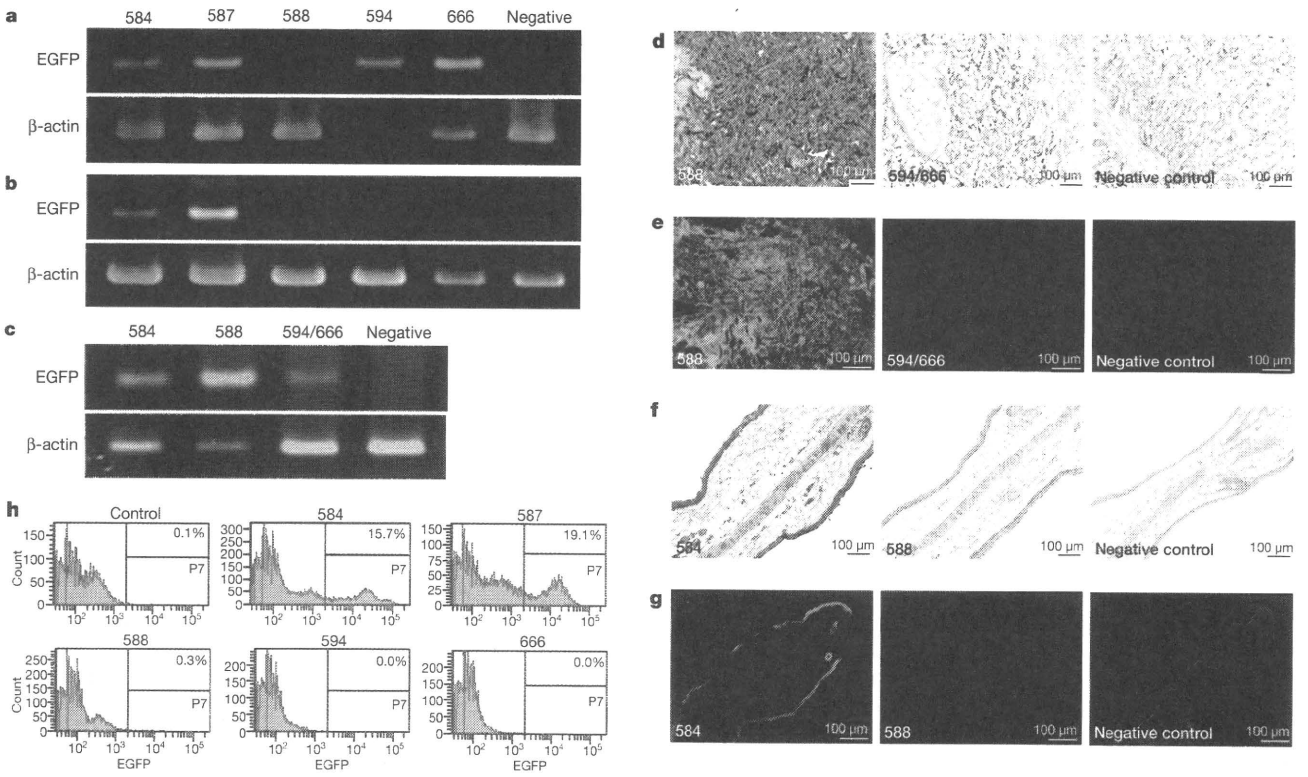

Figure 3 | Transgene transcription and expression in several infant tissues. **a–c**, RT–PCR results from hair roots (**a**), peripheral blood (**b**) and placenta (**c**). Each lane indicates the animal number. **d–g**, Immunohistochemical (**d**, **f**) and epifluorescence (**e**, **g**) analyses using an anti-EGFP antibody, of frozen ear tissues (**f**, **g**) and placentae (**d**, **e**). Scale bars, 100 μm. **h**, Results of FACS analysis using whole peripheral blood cells. The percentage of EGFP-positive cells is shown in the top right of each panel.

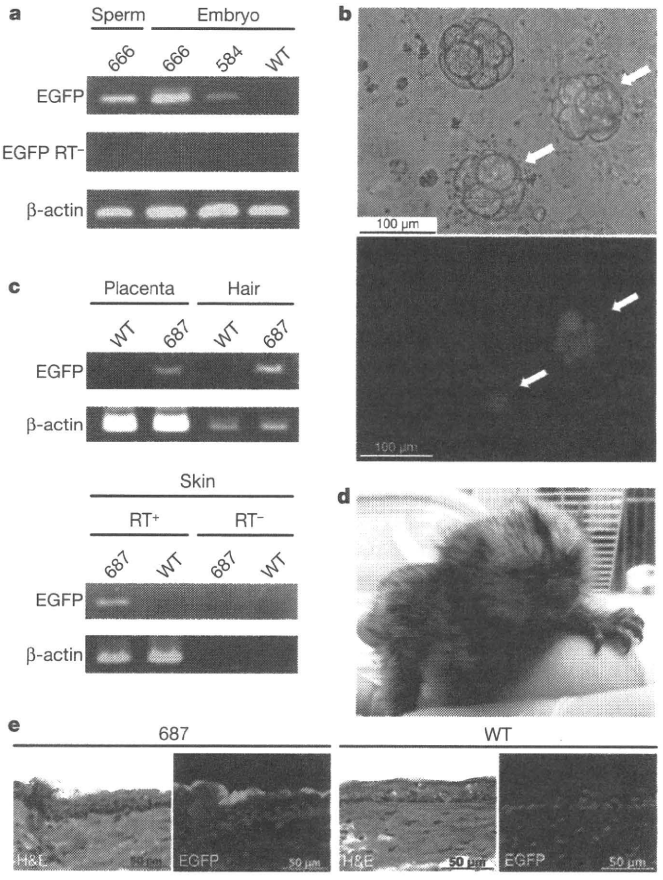

Figure 4 | Germline transmission of the transgene. **a**, RT–PCR analysis of spermatozoa and IVF embryos from 666, and natural embryos from 584. RT− denotes the absence of reverse transcriptase as a control. **b**, Bright-field and dark-field of epifluorescence images of IVF embryos. EGFP-positive IVF embryos produced with 666 spermatozoa are indicated by white arrows. **c**, PCR (top panel) and RT–PCR (bottom panel) analysis of the tissues from the F_1 neonate. **d**, Photograph of the F_1 offspring (687) from 666. **e**, Haematoxylin and eosin (H&E) staining and epifluorescence imaging of frozen skin tissue from the neonate. WT, wild-type control.

development of the embryo. We obtained five transgenic marmosets, four of which expressed the transgene in several somatic cell lineages, such as hair root, skin fibroblast and peripheral blood cells. The remaining animal expressed the transgene only in the placenta. Two of these animals reached sexual maturity and showed the transgene insertion and expression in germ cells. Epifluorescence microscopic observation and RT–PCR analysis of embryos generated by transgene-bearing gametes strongly indicated that the transgenic germ cells from animals 666 and 584 were fertile, and this was proved for the male (666) who fathered one healthy, transgenic infant (687) with the transgene expression in the somatic cells. These findings suggest that it should be possible to establish transgenic non-human primate colonies, opening the door to their use in biomedical research.

Because the manipulation of embryos for viral injection and their subsequent culture may affect embryonic development, the birth rate after embryo transfer (6.25%) was lower than that for normal embryos (30.7%, data not shown). The miscarriage rates were not significantly different between embryonic transfers performed using normal embryos (28.6%) and transgenic embryos (42.6%). Despite considerable effort, transgenic marmosets have not been produced by DNA pronuclear microinjection. The production rate that we obtained using lentivirus (5.26–6.25%) suggests that our technique is sufficiently effective for the production and use of genetically modified marmosets as human disease models.

The 100% birth rate of transgenic marmosets achieved in the present study could be due to several technical advantages. First, we used EGFP as the transgene, enabling us to monitor the presence and expression of the transgene at each experimental step in live embryos and the transgenic animals. Accordingly, we were able to select unambiguously EGFP-expressing embryos for transfer into surrogate mothers. This selection was effective, not only for increasing the birth rate of transgenic animals, but also for reducing the number of surrogate mother animals needed.

Second, we used pre-implantation embryos obtained by natural intercourse, high-titre lentiviral vectors, and 0.25 M sucrose solution as a medium for injection. Even though the birth rates (birth per embryonic transfer) were no different between IVF and natural embryos, the fertilization rate of the germinal vesicle-stage oocytes was quite low. Because it is difficult to collect large quantities of oocytes, it was advantageous to use marmoset natural embryos. To inject as much lentiviral vector as possible into the perivitelline space, the embryos were placed in 0.25 M sucrose medium at the time of lentiviral vector injection, which expanded the volume of the perivitelline space 1.2–7.5-fold. For example, the estimated volume of the perivitelline space of one marmoset pronuclear stage embryo was approximately 31.5 pl, but when placed in 0.25 M sucrose medium, it expanded to about 231 pl. A high titre of the lentiviral vector solution was used so that many lentiviral vector particles were injected into the expanded perivitelline space; approximately 1.3×10^3–1.3×10^5 transducing units of lentiviral vector were injected in this study. Each of these steps probably contributed to the successful production of transgenic marmosets.

The high number of injected lentiviral vector particles resulted in several transgene integrations, as observed by Southern blot analysis and FISH. The embryos injected with the transgene before the four-cell stage (584 and 587) showed fewer than four copies of the transgene per genome by Southern blotting and FISH. The three other embryos (588, 594 and 666), which received the injection at the morula stage, exhibited several integrations of the transgene by Southern blotting and FISH. As the FISH analysis was performed using only peripheral blood MNCs, other patterns of transgene integration cells may have existed in other tissues. The FISH results for 666 were consistent with this hypothesis, as the integration sites in the chimaeric blood MNCs from his twin, 594, were different from those in the blood MNCs of 594.

The lentiviral vector used in the present study can be used to transmit only relatively small transgenes, 8.5 kilobases of DNA or less. Therefore, further study will be necessary to enable the introduction of larger transgenes into marmoset embryos. Furthermore, to study human diseases involving the malfunctions of specific genes, targeted gene-knockdown marmosets could be developed using RNA interference (RNAi) lentiviruses.

The results of the present study indicate that transgenic marmosets may be used as experimental animals for biomedical research. Recently, somatic cell nuclear-transferred embryonic stem cells from the rhesus macaque and induced pluripotent stem cells from adult human fibroblasts were reportedly established[12–15]. Those studies indicated that the obstacle caused by immunogenetic incompatibility has at least theoretically been resolved, and that a new era of regenerative medicine using somatic cell nuclear-transferred embryonic stem cells in primates[14] or human induced pluripotent stem cells[12,13,15] has become possible. However, before such stem cells can be used in clinical applications, preclinical assessments of their safety and efficacy are essential. We previously reported that marmosets with injured spinal cords can recover motor function after the transplantation of human neural stem/progenitor cells[16], highlighting the usefulness of the marmoset for assessing the safety and efficacy of, not only these cells, but also of other stem cells, such as human embryonic stem cells[17] or induced pluripotent stem cells. Human disease models in non-human primates have so far been limited to mechanical injury models (for example, spinal cord injury[18]) and drug administration models (for example, MPTP-induced Parkinson's[19,20]). The only transgene-induced primate disease model is of Huntington's disease[7], in rhesus

monkeys expressing a mutant human huntingtin gene. In that report, although the transgene was inserted into the genome of founder infants and its expression was detected in post-mortem animals, the germline transmission of the transgene has not yet been confirmed[7]. Thus, at this point, it is not certain how reproducible the effects of various therapeutic interventions would be using a large number of animals.

The technique by which we achieved transgene expression in several tissues, along with germline transmission, may provide the means to obtain genetically modified non-human primate models for translational research, investigations of regenerative medicine and gene therapy, and clarification of the scientific gaps among transgenic mice, human disease models, and real human diseases.

METHODS SUMMARY

All animal experiments were approved by the institutional animal care and use committee, and were performed in accordance with Central Institution for Experimental Animal (CIEA) guidelines.

To obtain oocytes, recombinant human follicle stimulating hormone (r-hFSH; 50 international units (IU); Fertinome, Serono) was administered daily by intramuscular injection for 11 days. Human chorionic gonadotropin (hCG; 75 IU; Gonatropin, Teikoku-zouki) was administered by intramuscular injection at 17:30 on day 12. On day 13, the animals were anaesthetized and follicular aspiration was performed surgically. Oocytes were incubated for 24 h at 38 °C, 5% CO_2 in air, for *in vitro* maturation. After incubation, only matured oocytes (metaphase II) were collected and used for IVF.

Ejaculated semen was collected in TYH medium (Mitsubishi Kagaku Iatron), using a Ferti Care personal vibrator. Hyaluronidase-treated oocytes were placed in 70-μl drops of TYH, and an aliquot of sperm (4×10^5) was added to each oocyte incubation drop. After 26–30 h of insemination, the fertilized oocytes were placed into ISM1 (Medicult) medium, and lentiviral vector injection was performed in 0.25 M sucrose.

Natural embryo collection was performed as previously described[21]. Embryos at the pronuclear-to-morula stage were placed in 0.25 M sucrose supplemented PB1 medium (Mitsubishi Chemical Medience Corporation) and injected with lentiviral vector. Blastocysts were not treated with sucrose. Lentiviral vector injection was performed using an Eppendorf FemtoJet express and a Narishige micromanipulator. The embryos were cultured until GFP expression was confirmed.

The ovulation cycles of donor and recipient animals were synchronized, and EGFP-expressing embryos were transferred as previously described[22,23]. After embryo transfer, the recipients were tested for pregnancy by plasma progesterone once a week. The resulting infants were analysed for transgene integration, transcription and expression, by real-time PCR, Southern blot analysis, RT–PCR, immunohistochemical analysis, FACS and FISH.

Full Methods and any associated references are available in the online version of the paper at www.nature.com/nature.

Received 27 September 2008; accepted 30 April 2009.

1. Mansfield, K. Marmoset models commonly used in biomedical research. *Comp. Med.* **53**, 383–392 (2003).
2. Chan, A. W., Homan, E. J., Ballou, L. U., Burns, J. C. & Bremel, R. D. Transgenic cattle produced by reverse-transcribed gene transfer in oocytes. *Proc. Natl Acad. Sci. USA* **95**, 14028–14033 (1998).
3. Hofmann, A. *et al.* Efficient transgenesis in farm animals by lentiviral vectors. *EMBO Rep.* **4**, 1054–1060 (2003).
4. Hofmann, A. *et al.* Generation of transgenic cattle by lentiviral gene transfer into oocytes. *Biol. Reprod.* **71**, 405–409 (2004).
5. Chan, A. W., Chong, K. Y., Martinovich, C., Simerly, C. & Schatten, G. Transgenic monkeys produced by retroviral gene transfer into mature oocytes. *Science* **291**, 309–312 (2001).
6. Wolfgang, M. J. *et al.* Rhesus monkey placental transgene expression after lentiviral gene transfer into preimplantation embryos. *Proc. Natl Acad. Sci. USA* **98**, 10728–10732 (2001).
7. Yang, S. H. *et al.* Towards a transgenic model of Huntington's disease in a non-human primate. *Nature* **453**, 921–924 (2008).
8. Rogers, C. S. *et al.* Disruption of the *CFTR* gene produces a model of cystic fibrosis in newborn pigs. *Science* **321**, 1837–1841 (2008).
9. Rogers, C. S. *et al.* Production of *CFTR*-null and *CFTR-ΔF508* heterozygous pigs by adeno-associated virus-mediated gene targeting and somatic cell nuclear transfer. *J. Clin. Invest.* **118**, 1571–1577 (2008).
10. Miyoshi, H., Blomer, U., Takahashi, M., Gage, F. H. & Verma, I. M. Development of a self-inactivating lentivirus vector. *J. Virol.* **72**, 8150–8157 (1998).
11. Ross, C. N., French, J. A. & Orti, G. Germ-line chimerism and paternal care in marmosets (*Callithrix kuhlii*). *Proc. Natl Acad. Sci. USA* **104**, 6278–6282 (2007).
12. Takahashi, K. *et al.* Induction of pluripotent stem cells from adult human fibroblasts by defined factors. *Cell* **131**, 861–872 (2007).
13. Yu, J. *et al.* Induced pluripotent stem cell lines derived from human somatic cells. *Science* **318**, 1917–1920 (2007).
14. Byrne, J. A. *et al.* Producing primate embryonic stem cells by somatic cell nuclear transfer. *Nature* **450**, 497–502 (2007).
15. Nakagawa, M. *et al.* Generation of induced pluripotent stem cells without Myc from mouse and human fibroblasts. *Nature Biotechnol.* **26**, 101–106 (2008).
16. Iwanami, A. *et al.* Transplantation of human neural stem cells for spinal cord injury in primates. *J. Neurosci. Res.* **80**, 182–190 (2005).
17. Thomson, J. A. *et al.* Embryonic stem cell lines derived from human blastocysts. *Science* **282**, 1145–1147 (1998).
18. Iwanami, A. *et al.* Establishment of graded spinal cord injury model in a nonhuman primate: the common marmoset. *J. Neurosci. Res.* **80**, 172–181 (2005).
19. Eslamboli, A. Marmoset monkey models of Parkinson's disease: which model, when and why? *Brain Res. Bull.* **68**, 140–149 (2005).
20. Ando, K. *et al.* Neurobehavioral protection by single dose l-deprenyl against MPTP-induced parkinsonism in common marmosets. *Psychopharmacology (Berl.)* **195**, 509–516 (2008).
21. Sasaki, E. *et al.* Establishment of novel embryonic stem cell lines derived from the common marmoset (*Callithrix jacchus*). *Stem Cells* **23**, 1304–1313 (2005).
22. Lopata, A., Summers, P. M. & Hearn, J. P. Births following the transfer of cultured embryos obtained by *in vitro* and *in vivo* fertilization in the marmoset monkey (*Callithrix jacchus*). *Fertil. Steril.* **50**, 503–509 (1988).
23. Summers, P. M., Shephard, A. M., Taylor, C. T. & Hearn, J. P. The effects of cryopreservation and transfer on embryonic development in the common marmoset monkey, *Callithrix jacchus*. *J. Reprod. Fertil.* **79**, 241–250 (1987).

Supplementary Information is linked to the online version of the paper at www.nature.com/nature.

Acknowledgements We thank F. Toyoda, S. Ohba, T. Inoue, Y. Sawada and M. Yokoyama for technical assistance with the animal experiments and care. E.S. is an associate professor of the Global COE program for human metabolomic systems biology assigned to Keio University. This study was also supported by the Global COE program for Education and Research Centre for Stem Cell Medicine from the Ministry of Education, Culture, Sports, Science and Technology (MEXT), the Japanese Government to Keio University. This study was also supported by funds from Solution-Oriented Research for Science and Technology (SORST) of the Japan Science and Technology Agency and grants from MEXT to H.O. and from Special Coordination Funds for Promoting Science and Technology of MEXT to S.H.

Author Contributions E.S. designed the experiments, conducted the project, and wrote the paper. A.S., Y.S., T.E., I.T. and R.H. assisted in embryological technique development. K.H., R.O. and M.K. developed surgical techniques for embryo collection and transfer. H.S., C.K. and C.Y. performed or assisted with the real-time PCR and parentage evaluation test. S.S. and T.M. assisted with the Southern blot analysis and tissue collection. M.I. raised the anti-marmoset CD45 antibody. R.I. performed the FACS analysis, and K.K. performed the immunohistochemical analysis. H.M. provided the lentiviral vectors. Y.T., H.O., S.H., N.T. and T.N. designed the project, and H.O., S.H. and N.T. also participated in writing the paper. The whole project was supervised by E.S. and H.O.

Author Information Reprints and permissions information is available at www.nature.com/reprints. Correspondence and requests for materials should be addressed to E.S. (esasaki@ciea.or.jp) or H.O. (hidokano@sc.itc.keio.ac.jp).

[RNA Biology 5:4, 1-5; October/November/December 2008]; ©2008 Landes Bioscience

Point of View

Newly identified ADAR-mediated A-to-I editing positions as a tool for ALS research

Shin Kwak,[1,*] Yoshinori Nishimoto[1,2] and Takenari Yamashita[1]

[1]Department of Neurology; Graduate School of Medicine; University of Tokyo; Bunkyo-ku, Tokyo Japan; [2]Department of Neurology; Graduate School of Medicine, Keio University; Shinjuku-ku, Tokyo Japan

Abbreviations: 5HT, 5-hytroxytryptamine (serotonine); ADAR, adenosine deaminase acting on RNA; ALS, amyotrophic lateral sclerosis; AMPA, alpha-amino-3-hydroxy-5-methyl-4-isoxazolepropionic acid; BLCAP, bladder cancer associated protein; CYFIP2, cytoplasmic fragile X mental retardation protein interacting protein 2; DRPLA, dentatorubro-pallidoluysian atrophy; FLNA, filamin A; hnRNP, heterogeneous nuclear ribonucleoprotein; IGFBP7, insulin-like growth factor binding protein 7; IP, immunoprecipitation; MND, motor neuron disease; PBP, progressive bulbar palsy; RNAi, RNA interference; SBMA, spinal and bulbar muscular atrophy; SCD, spinocerebellar degeneration; SOD1, Cu/Zn superoxide dismutase; TDP-43, transactivation response region DNA-biding protein 43

Key words: RNA editing, ADAR, GluR2, ALS, cell death

Among the extensively occurring adenosine to inosine (A-to-I) conversions in RNA, RNA editing at the GluR2 Q/R site is crucial for the survival of mammalian organisms. Editing at this site is incomplete in the motor neurons of patients with sporadic amyotrophic lateral sclerosis (ALS). Adenosine deaminase acting on RNA type 2 (ADAR2) specifically mediates GluR2 Q/R site-editing, hence, it is likely a molecule relevant to the pathogenesis of sporadic ALS. Since no other transcript with ADAR2-mediated A-to-I positions is abundantly expressed in most neurons, the editors at the newly identified A-to-I positions were investigated. CYFIP2 and FLNA mRNAs were identified together with mRNAs having known ADAR2-mediated editing positions in ADAR2-immunoprecipitates of the human cerebellum, indicating that these mRNAs probably possessed ADAR2-mediated positions. Furthermore, an in vitro RNAi knockdown system demonstrated that the CYFIP2 mRNA K/E site and the BLCAP mRNA Y/C site were edited predominantly by ADAR2 and ADAR1, respectively. CYFIP2 mRNA was ubiquitously expressed and particularly abundant in the central nervous system. The extent of CYFIP2 K/E site-editing was between 30% and 80% in the central nervous system. Therefore, the extent of CYFIP2 K/E site-editing may be an additional marker for ADAR2 activity in neuronal and other types of cells in vivo, as well as in vitro, and thus is considered to be a good tool for sporadic ALS research.

A-to-I RNA editing alters the stability, transport or processing of RNA, thereby enhancing the diversity of rather limited genetic information in a region- and even cell type-specific manner. A-to-I conversion occurs most extensively in vertebrate brains and the vast majority occurs in non-coding RNA regions, particularly in the inversely oriented repetitive elements including Alu sequences.[1-3] The important roles of non-coding RNA editing was recently demonstrated in an miRNA system with the alteration of miRNA processing by Drosha-DGCR8 and the generation of new miRNA targeting mRNAs that were different from those targeted by unedited miRNA.[2,4] A-to-I conversion in the coding region of RNA may alter the properties of transmitter-gated ion channels by substituting one amino acid to another as seen in Q/R site-editing of the glutamate receptor subunit.[5] In vertebrates, three structurally related ADARs (ADAR1, ADAR2 and ADAR3) have been identified as enzymes catalyzing the A-to-I conversion. ADAR1 mRNA is widely expressed in various organs where both larger (150-kDa) and smaller (110-kDa) ADAR1 proteins are produced by alternative splicing. ADAR1 is essential for normal development and ADAR1-null mice die in the early embryonic stages.[6] ADAR2 mRNA is widely expressed, most abundantly in the nervous system (Affymetrix HG-U133A:203865_s_at)[7-10] localized in the nucleus. One ADAR2 protein isoform was detected in the mouse brain,[11] whereas alternative splicing of the Alu sequence-containing exon generates two isoforms, ADAR2a and ADAR2b, with a greater abundance in the latter in the human cerebellum.[12] There are limited numbers of A-to-I positions specifically edited by either ADAR1 or ADAR2 in the coding RNA. An investigation on the brains of heterozygous ADAR1-null mice and homozygous ADAR2-null mice indicated that ADAR1 specifically mediates A-to-I conversion of the $5HT_{2c}$ receptor A site,[13,14] while ADAR2 specifically mediates that of the GluR2 Q/R site and the $5HT_{2c}$ receptor C and D sites.[15-25] Recent investigations on the brains of knockout mice and cultured cells using the RNAi system added a new ADAR1-selective A-to-I position in BLCAP mRNA, and the ADAR2-selective positions in mRNAs of CYFIP2 and FLNA.[10,26] ADAR3, a structurally related isoform of ADAR1 and ADAR2, is specifically expressed in the brain but no editing activity

*Correspondence to: Shin Kwak; Department of Neurology; Graduate School of Medicine; University of Tokyo; 7-3-1 Hongo; Bunkyo-ku, Tokyo 113-8655 Japan; Tel.: +81.3.5800.8672; Fax: +81.5800.8648; Email: kwak-tky@umin.ac.jp

Submitted: 05/02/08; Accepted: 09/05/08

Previously published online as an *RNA Biology* E-publication: http://www.landesbioscience.com/journals/mabiology/article/6925

has been demonstrated in either naturally occurring or artificial substrates.[27,28]

Diseases Associated with Anomalous RNA Editing

A-to-I conversion occurs most extensively in the central nervous system, thereby regulating the expression and properties of receptor/ion channels and the activities of neuronal circuits. Therefore, anomalous RNA editing may result in an abnormal phenotype leading to animal or human diseases affecting the central nervous system.

RNA editing at five A-to-I positions in the 5-hydroxytryptamine 2c (5-HT_{2c}) receptor changes the G-protein-coupled signal transduction in the downstream of the receptor activation and an increase of the extent of editing at the A or the E site has been demonstrated in patients with major depression and in a rat model of depression.[16,17,19,29,30] The editing of A-to-I positions in the 5-HT_{2c} receptor was observed to increase in the victims of suicide among patients with depression or schizophrenia, thus suggesting that 5-HT_{2c} receptor mRNA editing may be associated with changes in mood but not with comorbid psychiatric illnesses.[31] Indeed, the extent of RNA editing at these sites differs among mouse strains and was altered after the administration of antidepressants or exposure to a stressful environment in normal mouse brains.[16,32,33]

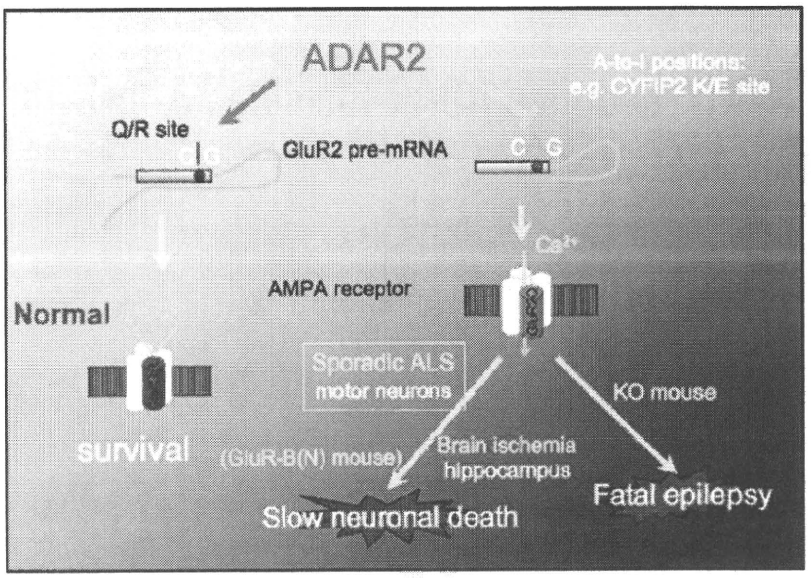

Figure 1. ADAR2 and GluR2 Q/R site-editing. AMPA receptors consist of tetrameric assembly of four subunits and their majority is impermeable to Ca^{2+} because Q/R site-edited GluR2 is included in its assembly. ADAR2 specifically edit the Q/R site of GluR2 pre-mRNA, and a reduction of its activity upregulate Ca^{2+} permeable AMPA receptors with Q/R site-unedited GluR2, which is toxic to neurons. ADAR2 knockout mice exhibit fatal epilepsy, but focal deficiency of ADAR2 activity induces slow neuronal death as seen in motor neurons of sporadic ALS patients and hippocampal pyramidal cells in rats after focal brain ischemia.

An A-to-I conversion of glutamate receptor subunits markedly alters the channel properties of glutamate receptors and hence, the neuronal excitability as a whole. In particular, mutant mice deficient in Q/R site-RNA editing of the AMPA receptor GluR2 subunit exhibit refractory epilepsy and those deficient in Q/R site-editing of the kainate receptor GluR6 subunits become susceptible to epilepsy, as a consequence of an increase of neuronal excitability due to increased Ca^{2+} permeability of these receptors.[34,35] However, no consistent results have been demonstrated as to alteration in editing at these sites in the brains of patients with refractory temporal lobe epilepsy.[36,37]

Several mutations have been identified in the ADAR1 gene in association with family members affected with dyschromatosis symmetrica hereditaria, a dermatologic disease with autosomally dominant transmission.[38] However, whether this skin-affecting disease is induced by a loss of ADAR1 editing function or by a gain of function of the mutated ADAR1 gene has not been demonstrated. Indeed, homozygous ADAR1-null mice die at early embryonic stage and heterozygous ADAR1-null mice are phenotypically normal.[6]

In contrast, motor neurons of patients with sporadic amyotrophic lateral sclerosis (ALS) express Q/R site-unedited GluR2 mRNA in variable proportions in a disease-specific and motor neuron-selective manner.[39]

ALS is the most common adult-onset motor neuron disease, characterized by progressive weakness and muscle wasting leading to death within a few years after onset due to the degeneration of both the upper and lower motor neurons. ALS affects healthy subjects abruptly in their mid-life with an incidence of around 1–3 in 100,000 every year. The majority of ALS cases are sporadic, with a variety of phenotypes including limb-onset classical ALS, progressive bulbar palsy (PBP) and ALS with dementia (ALS-D or FTD-MND). About 5–10% of ALS cases are familial, including Cu/Zn superoxide dismutase gene (SOD1)-associated familial ALS (ALS1) that accounts for about 20%, but none of the currently identified gene mutations has been demonstrated to be involved in sporadic ALS. The motor neurons of sporadic ALS patients express various proportions (ranging from 0% to 100%) of GluR2 mRNA lacking A-to-I conversion at the Q/R site.[39] Because inosin in mRNA is read as guanosine during translation, an A-to-I conversion in the Q/R site of GluR2 results in conversion of glutamine (Q:CAG) to arginine (R:CGG), thereby reducing the Ca^{2+} permeability of AMPA receptors containing GluR2 in their tetrameric subunits.[5] The majority of neurons express only Q/R site-edited GluR2 under normal conditions and if A-to-I conversions at this site are incomplete or abolished in artificial conditions, neurons became easily excitable due to an increase in Ca^{2+} influx through AMPA receptors and animals exhibited fatal status epilepticus[34] (Fig. 1). Furthermore, mice transgenic for GluR-B(N), an artificial gene encoding GluR2 with asparagine (N) at the Q/R site, developed motor deficit with a loss of motor neurons after 12 months of age.[40] Because GluR2 with N at the Q/R site works as Q/R site-unedited GluR2 in terms of Ca^{2+} permeability,[41] the results indicate that a substantial increase of Ca^{2+} permeability of AMPA receptors may induce slow progressive death at least in motor neurons (Fig. 1).

Although AMPA receptor-mediated neurotoxicity may play a role in ALS1 as well,[40,42,43] the underlying mechanism is not an increase of Q/R site-unedited GluR2-containing Ca^{2+} permeable AMPA receptors[44] (Table 1) unlike in sporadic ALS, but is likely due to an

Table 1 GluR2 Q/R site-editing in diseases

GluR2 mRNA Q/R site	Cortex (%)	motor neurons (%)	cbl/Purkinje cell (%)	hippocampus/pyramidal cells (%)	WM/glial cells (%)
normal human brain[20-25,39]	95–100	100	98–100	100	65–99
sporadic ALS[25,39]	95–100	0–100	98–100	ND	ND
SBMA[44]	ND	100	ND	ND	ND
SCD (DRPLA/MSA)[20,39]	ND	ND	98–100	ND	ND
malignant glioma[61,62]	ND	ND	ND	ND	69–88
normal rat[44,52]	100	100	100	100, 97	100
mSOD1-transgenic rat(G93A, H46R)[44]	ND	ND	100	ND	ND
rat transient forebrain ischemia[52]	ND	ND	ND	7–98	ND

increase of GluR2-lacking Ca^{2+} permeable AMPA receptors. Because GluR2 knockout mice did not display any neuronal death,[45] an increase of GluR2-lacking AMPA receptors per se cannot induce neuronal death and may be an exacerbating factor of excitotoxic neuronal death.[46] Neurotoxicity in mice deficient in GluR2 Q/R site-editing is likely due to an increased density of functional Ca^{2+} permeable AMPA receptors on the synaptic surface resulting from the facilitation of Q/R site-unedited GluR2-containing receptor trafficking.[47,48]

RNA editing at the GluR2 Q/R site is specifically catalyzed by ADAR2 in vertebrates.[15] ADAR2-null mice exhibit fatal status epilepticus[15] as do the mutant mice deficient in GluR2 Q/R site-editing,[34] but these mice display normal behavior when Q/R site-edited GluR2 without ADAR2 activity is expressed by crossing with mutant mice carrying the genetically engineered GluR2 gene encoding arginine (R) instead of glutamine (Q).[15] Therefore, the epileptogenic role of deficient ADAR2 seems to be solely due to deficient editing at the GluR2 Q/R site among various A-to-I positions in both coding[15,49-51] and non-coding RNAs.[4] A reduction of ADAR2 activity in a subset of neurons induces slow progressive neuronal death as demonstrated in the delayed neuronal death of rat hippocampal pyramidal cells after transient ischemia[52] and in the slow progressive death of motor neurons in a conditional ADAR2 knockout mouse.[53] Therefore, the reduction in GluR2 Q/R site-editing in motor neurons of sporadic ALS is likely due to ADAR2 underactivity.[20] Indeed, the expression level of ADAR2 mRNA relative to GluR2 mRNA, a determinant of ADAR2 activity in human white matter,[18] is markedly reduced in the spinal ventral gray matter of sporadic ALS patients,[20,54] thus indicating a reduction of the ADAR2 activity in motor neurons. To demonstrate ADAR2 underactivity in motor neurons of sporadic ALS, a reduction in more than one A-to-I positions that are specifically mediated by ADAR2 may be necessary. However, other than the GluR2 Q/R site, no ADAR2-specific A-to-I position has yet been identified in mRNAs expressed abundantly in the motor neurons.

Novel A-to-I Positions and their Editors

Recently, computational genomic approaches and bioinformatics screening have demonstrated novel A-to-I conversions in four different mRNAs; cytoplasmic fragile X mental retardation protein interacting protein 2 (CYFIP2), filamin A (FLNA), bladder cancer associated protein (BLCAP) and insulin-like growth factor binding protein 7 (IGFBP7).[55] These mRNAs were investigated for specifically ADAR2- or ADAR1-mediated positions because determination of editors at novel A-to-I positions would be useful for analyzing ADARs activities in vivo. An immunoprecipitation (IP) method and an in vitro RNAi knockdown system of ADAR1 and ADAR2 demonstrated that the K/E site in CYFIP2 mRNA and the Y/C site in BLCAP mRNA are edited predominantly by ADAR2 and ADAR1, respectively, and the Q/R site in FLNA mRNA is possibly edited by ADAR2.[10] In brief, CYFIP2, FLNA, GluR2 and kv1.1 mRNAs but not β-actin, BLCAP or IGFBP7 mRNA were recovered from an ADAR2-immunoprecipitate of the nuclear fraction of human cerebellum. Because GluR2 and kv1.1 mRNAs, but not b-actin mRNA, have ADAR2-mediated editing positions, these results suggest that CYFIP2 and FLNA mRNAs, but not BLCAP or IGFBP7 mRNA, have ADAR2-mediated positions. Indeed, in vitro knockdown experiments indicated that the K/E site in CYFIP2 mRNA and the Y/C site in BLCAP mRNA are catalyzed mainly by ADAR2 and ADAR1, respectively (Table 2). Jantsch's lab also reported consistent results from the analysis of the extent of editing by sequencing of cDNAs derived from ADAR2-null mouse brain and primary neuronal culture of ADAR1-null and ADAR1/ADAR2-null mice[26] (Table 2). In accordance with the prediction, they showed that the extent of FLNA Q/R site-editing in ADAR2 null mouse brains is lower than that in control mice. The consistency between the two reports using different methodology strongly suggests that ADAR2 predominantly mediates CYFIP2 K/E site- and FLNA Q/R site-editing and ADAR1 predominantly mediates BLCAP Y/C site- and IGFBP7 K/R site-editing.

A Tool for Sporadic ALS Research

Although normal human motor neurons express only Q/R site-edited GluR2 mRNA,[39] the relative abundance of ADAR2 mRNA markedly differed among neurons,[18] thus suggesting that GluR2 Q/R site-editing may be preserved even in neurons with a relatively low ADAR2 activity. Because the downregulation of the ADAR2 activity is likely an inducer of neuronal death, markers representing a wide range of ADAR2 activity may be a useful tool for detection of the disease onset and evaluation of the efficacy of therapy by ADAR2 upregulation. CYFIP2 mRNA is ubiquitously expressed and is particularly abundant in the central nervous system including motor neurons in the spinal cord (unpublished observation). The extent of CYFIP2 K/E site-editing are in the range of about 30% to 85% in the human brains and spinal cord.[10] Therefore, the extent of CYFIP2 K/E site-editing may become an additional marker for

Table 2 Novel A-to-I positions

	normal mouse brain[26] (%)	ADAR1$^{-/-}$ mouse primary culture[26] (%)	ADAR2$^{-/-}$ mouse brain[26] (%)	human cerebellum[10] (%)	ADAR1 siRNA[10] (%)	ADAR2 siRNA[10] (%)
CYFIP2 K/E site	90	→	↓11	84	↓	0
BLCAP Y/C site	50	↓	33.5	-30	0	→
FLNA Q/R site	16.5	→	↓13.5	0	ND	ND

ADAR2 activity in neuronal and other types of cells in vivo, as well as in vitro. Furthermore, since BLCAP mRNA is abundantly expressed in human brain tissue, the extent of BLCAP Y/C site-editing may become a marker for ADAR1 activity in vivo.

However, The extent of CYFIP2 K/E site-editing and ADAR2 mRNA expression level is not necessarily correlated among human tissues.[10] ADAR2 activity is influenced by several factors including the subcellular localization of ADAR2 protein,[56-58] inositol phosphate 6 (IP-6)[59] and glucose concentration[60]. ADAR2 activity on the GluR2 Q/R site-editing is reduced in human malignant glioma cells[61,62] in which ADAR1 overexpression might reduce the number of active ADAR2 homodimers by facilitating inactive ADAR1/ADAR2 hetero-dimer formation.[62-64] These results suggest that there may be cell type-specific and substrate-specific mechanisms underlying the regulation of ADAR2 activity. However, why ADAR2 is downregulated in motor neurons of sporadic ALS remains to be elucidated.

Recently, abnormally processed TAR DNA-binding protein 43 (TDP-43), a member of hnRNP playing a regulatory role in pre-mRNA splicing,[65-69] was demonstrated to accumulate in cytoplasmic inclusion bodies of motor neurons of patients with sporadic ALS as well as in the cortical neurons of those with frontotemporal lobar degeneration (FTLD),[70,71] but not in cytoplasmic inclusion bodies of motor neurons of patients with SOD1-associated familial ALS.[72,73] Therefore, it is likely that the death-inducing mechanism underlying sporadic ALS may be different from that underlying SOD1-associated familial ALS. On the other hand, several different missense mutations in the TDP-43 gene are found in patients with SOD1-unassociated familial ALS that is clinically and neuropathologically very similar to sporadic ALS.[74] The finding that these mutations were detected only in a small proportion of sporadic ALS cases[74-78] suggests that, although the mechanism underlying aberrant TDP-43 processing is different from TDP-43 gene mutation, the TDP-43 dysfunction resulting from either aberrant protein processing or gene mutation may induce a common neuronal death-inducing cascade. Due to the critical roles that the aberrant TDP-43 processing and ADAR2 under-activity played in the death of motor neurons, the elucidation of a link between these molecular abnormalities may provide a clue to the pathogenesis of sporadic ALS.

The upregulation of ADAR2 activity with normalization of GluR2 Q/R site-editing may become a strategy for ALS therapy, which includes drugs stimulating ADAR2 activity and ADAR2 gene transfer. In such settings, an analysis of RNA editing at newly demonstrated A-to-I positions in CYFIP2 and FLNA mRNA may become a useful tool for evaluating ADAR2 activity and the efficacy of the therapy in vivo, hence a key for opening the door to a cure that has been elusive for patients during the nearly 150 year-long history of ALS research.

References

1. Bass BL. RNA editing by adenosine deaminases that act on RNA. Annu Rev Biochem 2002; 71:817-46.
2. Nishikura K. Editor meets silencer: crosstalk between RNA editing and RNA interference. Nat Rev Mol Cell Biol 2006; 7:919-31.
3. Reenan RA. The RNA world meets behavior: A→I pre-mRNA editing in animals. Trends Genet 2001; 17:53-6.
4. Kawahara Y, et al. Redirection of silencing targets by adenosine-to-inosine editing of miRNAs. Science 2007; 315:1137-40.
5. Seeburg PH. A-to-I editing: new and old sites, functions and speculations. Neuron 2002; 35:17-20.
6. Wang Q, Khillan J, Gadue P and Nishikura K. Requirement of the RNA editing deaminase ADAR1 gene for embryonic erythropoiesis. Science 2000; 290:1765-8.
7. Mittaz L, et al. Cloning of a human RNA editing deaminase (ADARB1) of glutamate receptors that maps to chromosome 21q22.3. Genomics 1997; 41:210-7.
8. Gerber A, O'Connell M and W K. Two forms of human double-stranded RNA-specific editase 1 (hRED1) generated by the insertion of an Alu cassette. Rna 1997; 3:453-63.
9. Lai F, Chen C, Carter K and Nishikura K. Editing of glutamate receptor B subunit ion channel RNAs by four alternatively spliced DRADA2 double-stranded RNA adenosine deaminases. Mol Cell Biol 1997; 17:2413-24.
10. Nishimoto Y, et al. Determination of editors at the novel A-to-I editing positions. Neurosci Res 2008; 61:201-6.
11. Feng Y, Sansam CL, Singh M and Emeson RB. Altered RNA editing in mice lacking ADAR2 autoregulation. Mol Cell Biol 2006; 26:480-8.
12. Kawahara Y, Ito K, Ito M, Tauji S and Kwak S. Novel splice variants of human ADAR2 mRNA: Skipping of the exon encoding the dsRNA-binding domains, and multiple C-terminal splice sites. Gene 2005; 363:193-201.
13. Hartner JC, et al. Liver disintegration in the mouse embryo caused by deficiency in the RNA-editing enzyme ADAR1. J Biol Chem 2004; 279:4894-902.
14. Wang Q, et al. Stress-induced apoptosis associated with null mutation of ADAR1 RNA editing deaminase gene. J Biol Chem 2004; 279:4952-61.
15. Higuchi M, et al. Point mutation in an AMPA receptor gene rescues lethality in mice deficient in the RNA-editing enzyme ADAR2. Nature 2000; 406:78-81.
16. Gurevich I, et al. Altered editing of serotonin 2C receptor pre-mRNA in the prefrontal cortex of depressed suicide victims. Neuron 2002; 34:349-56.
17. Iwamoto K, Nakatani N, Bundo M, Yoshikawa T and Kato T. Altered RNA editing of serotonin 2C receptor in a rat model of depression. Neurosci Res 2005; 53:69-76.
18. Kawahara Y, Ito K, Sun H, Kanazawa I and Kwak S. Low editing efficiency of GluR2 mRNA is associated with a low relative abundance of ADAR2 mRNA in white matter of normal human brain. Eur J Neurosci 2003; 18:23-33.
19. Niswender CM, et al. RNA editing of the human serotonin 5-HT2C receptor. alterations in suicide and implications for serotonergic pharmacotherapy. Neuropsychopharmacology 2001; 24:478-91.
20. Kwak S and Kawahara Y. Deficient RNA editing of GluR2 and neuronal death in amyotropic lateral sclerosis. J Mol Med 2005; 83:110-20.
21. Akbarian S, Smith M and Jones E. Editing for an AMPA receptor subunit RNA in prefrontal cortex and striatum in Alzheimer's disease, Huntington's disease and schizophrenia. Brain Res 1995; 699:297-304.
22. Nutt S and Kamboj R. Differential RNA editing efficiency of AMPA receptor subunit GluR-2 in human brain. NeuroReport 1994; 5:1679-83.
23. Nutt S and Kamboj R. RNA editing of human kainate receptor subunits. NeuroReport 1994; 5:2625-9.
24. Paschen W, Hedreen J and Ross C. RNA editing of the glutamate receptor subunits GluR2 and GluR6 in human brain tissue. J Neurochem 1994; 63:1596-602.
25. Takuma H, Kwak S, Yoshizawa T and Kanazawa I. Reduction of GluR2 RNA editing, a molecular change that increases calcium influx through AMPA receptors, selective in the spinal ventral gray of patients with amyotrophic lateral sclerosis. Ann Neurol 1999; 46:806-15.
26. Riedmann EM, Schopoff S, Hartner JC and Jantsch MF. Specificity of ADAR-mediated RNA editing in newly identified targets. Rna 2008; 14:1110-8.
27. Melcher T, et al. RED2, a brain-specific member of the RNA-specific adenosine deaminase family. J Biol Chem 1996; 271:31795-8.

28. Chen CX, et al. A third member of the RNA-specific adenosine deaminase gene family, ADAR3, contains both single- and double-stranded RNA binding domains. Rna 2000; 6:755-67.
29. Schmauss C. Serotonin 2C receptors: suicide, serotonin and runaway RNA editing. Neuroscientist 2003; 9:237-42.
30. Iwamoto K and Kato T. RNA editing of serotonin 2C receptor in human postmortem brains of major mental disorders. Neurosci Lett 2003; 346:169-72.
31. Dracheva S, et al. Increased serotonin 2C receptor mRNA editing: a possible risk factor for suicide. Mol Psychiatry 2007.
32. Bhansali P, Dunning J, Singer SE, David L and Schmauss C. Early life stress alters adult serotonin 2C receptor pre-mRNA editing and expression of the alpha subunit of the heterotrimeric G-protein G q. J Neurosci 2007; 27:1467-73.
33. Englander MT, Dulawa SC, Bhansali P and Schmauss C. How stress and fluoxetine modulate serotonin 2C receptor pre-mRNA editing. J Neurosci 2005; 25:648-51.
34. Brusa R, et al. Early-onset epilepsy and postnatal lethality associated with an editing-deficient GluR-B allele in mice. Science 1995; 270:1677-80.
35. Vissel B, et al. The role of RNA editing of kainate receptors in synaptic plasticity and seizures. Neuron 2001; 29:217-27.
36. Grigorenko EV, Bell WL, Glazier S, Pons T and Deadwyler S. Editing status at the Q/R site of the GluR2 and GluR6 glutamate receptor subunits in the surgically excised hippocampus of patients with refractory epilepsy. NeuroReport 1998; 9:2219-24.
37. Kortenbruck G, Berger E, Speckmann EJ and Musshoff U. RNA editing at the Q/R site for the glutamate receptor subunits GLUR2, GLUR5 and GLUR6 in hippocampus and temporal cortex from epileptic patients. Neurobiol Dis 2001; 8:459-68.
38. Miyamura Y, et al. Mutations of the RNA-specific adenosine deaminase gene (DSRAD) are involved in dyschromatosis symmetrica hereditaria. Am J Hum Genet 2003; 73:693-9.
39. Kawahara Y, et al. Glutamate receptors: RNA editing and death of motor neurons. Nature 2004; 427:801.
40. Kuner R, et al. Late-onset motoneuron disease caused by a functionally modified AMPA receptor subunit. Proc Natl Acad Sci USA 2005; 102:5826-31.
41. Feldmeyer D, et al. Neurological dysfunctions in mice expressing different levels of the Q/R site-unedited AMPAR subunit GluR-B. Nat Neurosci 1999; 2:57-64.
42. Van Damme P, Braeken D, Callewaert G, Robberecht W and Van Den Bosch L. GluR2 deficiency accelerates motor neuron degeneration in a mouse model of amyotrophic lateral sclerosis. J Neuropathol Exp Neurol 2005; 64:605-12.
43. Tateno M, et al. Calcium-permeable AMPA receptors promote misfolding of mutant SOD1 protein and development of amyotrophic lateral sclerosis in a transgenic mouse model. Hum Mol Genet 2004; 13:2183-96.
44. Kawahara Y, et al. Underediting of GluR2 mRNA, a neuronal death inducing molecular change in sporadic ALS, does not occur in motor neurons in ALS1 or SBMA. Neurosci Res 2006; 54:11-4.
45. Jia Z, et al. Enhanced LTP in mice deficient in the AMPA receptor GluR2. Neuron 1996; 17:945-56.
46. Kwak S and Weiss JH. Calcium-permeable AMPA channels in neurodegenerative disease and ischemia. Curr Opin Neurobiol 2006; 16:281-7.
47. Mahajan SS and Ziff EB. Novel toxicity of the unedited GluR2 AMPA receptor subunit dependent on surface trafficking and increased Ca^{2+}-permeability. Mol Cell Neurosci 2007; 35:470-81.
48. Greger IH, Khatri L and Ziff EB. RNA editing at arg607 controls AMPA receptor exit from the endoplasmic reticulum. Neuron 2002; 34:759-72.
49. Burns CM, et al. Regulation of serotonin-2C receptor G-protein coupling by RNA editing. Nature 1997; 387:303-8.
50. Hoopengardner B, Bhalla T, Staber C and Reenan R. Nervous system targets of RNA editing identified by comparative genomics. Science 2003; 301:832-6.
51. Rueter SM, Dawson TR and Emeson RB. Regulation of alternative splicing by RNA editing. Nature 1999; 399:75-80.
52. Peng PL, et al. ADAR2-dependent RNA editing of AMPA receptor subunit GluR2 determines vulnerability of neurons in forebrain ischemia. Neuron 2006; 49:719-33.
53. Kwak S, et al. Development of a mouse model of sporadic ALS by deficient RNA editing. Neurosci Res 2007; 58 (Supple):S119.
54. Kawahara Y and Kwak S. Excitotoxicity and ALS: what is unique about the AMPA receptors expressed on spinal motor neurons? Amyotroph Lateral Scler Other Motor Neuron Disord 2005; 6:131-44.
55. Levanon EY, et al. Evolutionarily conserved human targets of adenosine to inosine RNA editing. Nucleic Acids Res 2005; 33:1162-8.
56. Desterro JM, et al. Dynamic association of RNA-editing enzymes with the nucleolus. J Cell Sci 2003; 116:1805-18.
57. Poulsen H, Nilsson J, Damgaard CK, Egebjerg J and Kjems J. CRM1 mediates the export of ADAR1 through a nuclear export signal within the Z-DNA binding domain. Mol Cell Biol 2001; 21:7862-71.
58. Sansam CL, Wells KS and Emeson RB. Modulation of RNA editing by functional nucleolar sequestration of ADAR2. Proc Natl Acad Sci USA 2003; 100:14018-23.
59. Macbeth MR, et al. Inositol hexakisphosphate is bound in the ADAR2 core and required for RNA editing. Science 2005; 309:1534-9.
60. Gan Z, et al. RNA editing by ADAR2 is metabolically regulated in pancreatic islets and beta-cells. J Biol Chem 2006; 281:33386-94.
61. Maas S, Patt S, Schrey M and Rich A. Underediting of glutamate receptor GluR-B mRNA in malignant gliomas. Proc Natl Acad Sci USA 2001; 98:14687-92.
62. Cenci C, et al. Downregulation of RNA Editing in Pediatric Astrocytomas: ADAR2 EDITING ACTIVITY INHIBITS CELL MIGRATION AND PROLIFERATION. J Biol Chem 2008; 283:7251-60.
63. Cho DS, et al. Requirement of dimerization for RNA editing activity of adenosine deaminases acting on RNA. J Biol Chem 2003; 278:17093-102.
64. Gallo A, Keegan LP, Ring GM and O'Connell MA. An ADAR that edits transcripts encoding ion channel subunits functions as a dimer. Embo J 2003; 22:3421-30.
65. Ayala YM, et al. Human, Drosophila and *C. elegans* TDP43: nucleic acid binding properties and splicing regulatory function. J Mol Biol 2005; 348:575-88.
66. Buratti E, Brindisi A, Pagani F and Baralle FE. Nuclear factor TDP-43 binds to the polymorphic TG repeats in CFTR intron 8 and causes skipping of exon 9: a functional link with disease penetrance. Am J Hum Genet 2004; 74:1322-5.
67. Buratti E, et al. Nuclear factor TDP-43 and SR proteins promote in vitro and in vivo CFTR exon 9 skipping. Embo J 2001; 20:1774-84.
68. Ayala YM, Pagani F and Baralle FE. TDP43 depletion rescues aberrant CFTR exon 9 skipping. FEBS Lett 2006; 580:1339-44.
69. Mercado PA, Ayala YM, Romano M, Buratti E and Baralle FE. Depletion of TDP 43 overrides the need for exonic and intronic splicing enhancers in the human apoA-II gene. Nucleic Acids Res 2005; 33:6000-10.
70. Arai T, et al. TDP-43 is a component of ubiquitin-positive tau-negative inclusions in frontotemporal lobar degeneration and amyotrophic lateral sclerosis. Biochem Biophys Res Commun 2006; 351:602-11.
71. Neumann M, et al. Ubiquitinated TDP-43 in frontotemporal lobar degeneration and amyotrophic lateral sclerosis. Science 2006; 314:130-3.
72. Mackenzie IR, et al. Pathological TDP-43 distinguishes sporadic amyotrophic lateral sclerosis from amyotrophic lateral sclerosis with SOD1 mutations. Ann Neurol 2007; 61:427-34.
73. Tan CF, et al. TDP-43 immunoreactivity in neuronal inclusions in familial amyotrophic lateral sclerosis with or without SOD1 gene mutation. Acta Neuropathol (Berl) 2007; 113:535-42.
74. Yokoseki A, et al. TDP-43 mutation in familial amyotrophic lateral sclerosis. Ann Neurol 2008; 63:538-42.
75. Van Deerlin VM, et al. TARDBP mutations in amyotrophic lateral sclerosis with TDP-43 neuropathology: a genetic and histopathological analysis. Lancet Neurol 2008; 7:409-16.
76. Kabashi E, et al. TARDBP mutations in individuals with sporadic and familial amyotrophic lateral sclerosis. Nat Genet 2008; 40:572-4.
77. Sreedharan J, et al. TDP-43 mutations in familial and sporadic amyotrophic lateral sclerosis. Science 2008; 319:1668-72.
78. Gitcho MA, et al. TDP-43 A315T mutation in familial motor neuron disease. Ann Neurol 2008; 63:535-8.

Acta Neuropathol
DOI 10.1007/s00401-010-0678-x

ORIGINAL PAPER

TDP-43 pathology in sporadic ALS occurs in motor neurons lacking the RNA editing enzyme ADAR2

Hitoshi Aizawa · Jun Sawada · Takuto Hideyama · Takenari Yamashita · Takayuki Katayama · Naoyuki Hasebe · Takashi Kimura · Osamu Yahara · Shin Kwak

Received: 20 October 2009 / Revised: 28 February 2010 / Accepted: 20 March 2010

Abstract Both the appearance of cytoplasmic inclusions containing phosphorylated TAR DNA-binding protein (TDP-43) and inefficient RNA editing at the GluR2 Q/R site are molecular abnormalities observed specifically in motor neurons of patients with sporadic amyotrophic lateral sclerosis (ALS). The purpose of this study is to determine whether a link exists between these two specific molecular changes in ALS spinal motor neurons. We immunohistochemically examined the expression of adenosine deaminase acting on RNA 2 (ADAR2), the enzyme that specifically catalyzes GluR2 Q/R site-editing, and the expression of phosphorylated and non-phosphorylated TDP-43 in the spinal motor neurons of patients with sporadic ALS. We found that all motor neurons were ADAR2-positive in the control cases, whereas more than half of them were ADAR2-negative in the ALS cases. All ADAR2-negative neurons had cytoplasmic inclusions that were immunoreactive to phosphorylated TDP-43, but lacked non-phosphorylated TDP-43 in the nucleus. Our results suggest a molecular link between reduced ADAR2 activity and TDP-43 pathology.

Keywords Amyotrophic lateral sclerosis · Adenosine deaminase acting on RNA 2 · TDP-43 · RNA editing · Motor neuron

Electronic supplementary material The online version of this article (doi:10.1007/s00401-010-0678-x) contains supplementary material, which is available to authorized users.

H. Aizawa · J. Sawada · T. Katayama · N. Hasebe
Division of Neurology, Department of Internal Medicine, Asahikawa Medical College, 2-1-1-1 Midorigaoka-higashi, Asahikawa 078-8510, Japan

T. Hideyama · T. Yamashita · S. Kwak (✉)
CREST, Japan Science and Technology Agency, Department of Neurology, Graduate School of Medicine, The University of Tokyo, 7-3-1, Hongo, Bunkyo-ku, Tokyo 113-8655, Japan
e-mail: kwak-tky@umin.net

T. Kimura · O. Yahara
Department of Neurology, Douhoku National Hospital, Asahikawa, Japan

Introduction

Amyotrophic lateral sclerosis (ALS) is a devastating disease characterized by a progressive deterioration of motor function resulting from the degeneration of motor neurons. More than 90% of ALS cases are sporadic and approximately 5–10% are familial. Although at least six causal genes have been identified so far in individuals affected with familial ALS, SOD1 [30], ALS2 (alsin) [10, 39], senataxin (ALS4) [7], vesicle-trafficking protein/synaptobrevin-associated membrane protein [27], TAR DNA-binding protein (TDP-43) [9, 15, 32, 37, 40] and FUS/TLS [22, 38], the pathogenesis of sporadic ALS remains largely unexplored.

One hypothesis for selective neuronal death in sporadic ALS is excitotoxicity mediated by abnormally Ca^{2+}-permeable α-amino-3-hydroxy-5-methyl-4-isoxazolepropionate (AMPA) receptors, which are a subtype of the ionotropic glutamate receptor [6, 20, 21]. The recent finding of reduced RNA editing of the AMPA receptor subunit GluR2 at the Q/R site provides a plausible pathogenic mechanism underlying motor neuron death in sporadic ALS [16, 21, 34]. Reduced GluR2 Q/R site-editing, catalyzed by an

Published online: 07 April 2010

enzyme called adenosine deaminase acting on RNA 2 (ADAR2), appears to be specific to sporadic ALS among several neurodegenerative diseases [1, 19, 20, 29, 33].

TDP-43 was identified as a component of ubiquitin-positive, but tau-negative cytoplasmic inclusions in cortical neurons in patients with frontotemporal lobar degeneration (FTD) and spinal motor neurons in patients with sporadic ALS [3]. The TDP-43 found in these inclusions was demonstrated to be abnormally phosphorylated [12, 26].

Because both reduced GluR2 Q/R site-editing and formation of TDP-43-containing inclusions occur specifically in sporadic ALS motor neurons, we used immunohistochemistry to examine the expression of TDP-43 and ADAR2 in ALS motor neurons and elucidate a link between these two molecules.

Materials and methods

Subjects

This study was conducted using lumbar spinal cords from seven cases of sporadic ALS and six disease-free control cases. Consent for autopsy and approval for the use of human tissue specimens for research purposes was approved by appropriate institutional human ethics committees. Clinical information is given in Table 1.

Western blot analysis using the anti-ADAR2 antibody (RED1)

To examine the specificity of the polyclonal anti-ADAR2 antibody (RED 1) (Exalpha Biologicals, Watertown, MA) in the human brain, Western blot analysis was performed as reported previously [17]. From 100 mg of human frontal cortex, nuclear and cytoplasmic fractions were separated with the PARIS Protein and RNA Isolation System (TAKARA, Tokyo) according to the manufacturer's instructions. Nuclear and cytoplasmic proteins as well as those containing recombinant ADAR2a (rADAR2a) and recombinant ADAR2b (rADAR2b) proteins synthesized by in vitro translation were suspended in 500 μl of cold Cell Fraction Buffer provided with the PARIS Protein and RNA Isolation System (TAKARA). Samples were then boiled with 500 μl of 2 × SDS gel-loading buffer and subjected to SDS-PAGE. After electrophoresis, proteins were transferred to an Immobilon-P transfer membrane (Millipore, Bedford, MA). Blots were blocked in a buffer containing Tween/PBS and 1% bovine serum albumin (BSA). Then immunoblotting for histone protein (MAB052; CHEMICON, Temecula, CA; 1:2,000), glyceraldehyde-3 phosphate dehydrogenase (GAPDH) (MAB374; CHEMICON, 1:2,000) or ADAR2 (RED1; Exalpha Biologicals, Watertown, MA, 1:4,000) was conducted overnight at 4°C. For secondary antibodies, peroxidase-conjugated AffiniPure goat anti-mouse IgG (H + L) (Jackson ImmunoResearch, West Grove, PA; 1:5,000) or peroxidase-conjugated AffiniPure rabbit anti-sheep IgG (H + L) (Jackson ImmunoResearch; 1:5,000) was used. Visualization was carried out using ECL plus Western blotting detection reagents (GE Healthcare Bioscience, Piscataway, NJ). Specific bands were detected with an LAS 3000 system (Fujifilm, Tokyo).

Immunohistochemical analysis

The human spinal cords were fixed in 10% neutral buffered formalin for about 7 days and then embedded in paraffin. Serial 7 μm sections were cut for immunohistochemical analysis. The immunoreactive features of the anti-ADAR2 antibody on frozen sections were also evaluated. To examine the localization of ADAR2 and TDP-43 in a single neuron, a pair of adjacent sections was used for immunohistochemistry. The sections were mounted on slides and then deparaffinized in xylene, hydrated with an ethanol series and heated at 120°C for 2 min for antigen retrieval. The sections were then washed with phosphate-buffered saline (PBS) and incubated with the primary antibody overnight at 4°C. Polyclonal anti-ADAR2 (RED1, 1:100), monoclonal anti-phosphorylated TDP-43 (pTDP-43) (pS409/410) (Cosmo Bio Co., Ltd., Tokyo, Japan; 1:3,000) and rabbit polyclonal phosphorylation-independent anti-TARDBP (piTDP-43) (Protein-Tech Group, Inc.; 1:3,000) were used. Bound antibodies were detected using an avidin–biotin–peroxidase complex kit (Vector Laboratories, Burlingame, CA, USA). Diaminobenzidine tetrahydrochloride was used as the chromogen, and the sections were lightly counterstained with hematoxylin. The RED1 antibody was incubated with 5 μg/μl of recombinant ADAR2 (Abnova Corp., Taiwan) at 4°C overnight. These samples were then subjected to immunohistochemistry for the preabsorption test.

To test the effects of fixation, the paraffin-embedding procedure and the postmortem delay on ADAR2 immunoreactivity, rat spinal cord samples were processed either immediately after removal (PMI-0) or after the spinal cords were held at room temperature for 6 h (PMI-6) or 24 h (PMI-24). Some samples were quickly frozen on dry ice, and the others were fixed in 10% buffered formalin after each treatment. The immunohistochemical process was the same as that used for the paraffin-embedded human sections, except that frozen sections were incubated with the primary antibody for 1 h at room temperature after washing with PBS.

Frozen sections of lumbar spinal cords from SOD1^{G93A} transgenic mice at 24 and 35 weeks of age were also used for immunohistochemistry with anti-ADAR2 and anti-pTDP-43 antibodies.

Table 1 Profiles of ALS cases and disease controls

Case	Age	Sex	PMI (h)	Brain weight (g)	Diagnosis	Duration of ALS	Onset of ALS	Number of MN/AH mean ± SD	ADAR2 (+) pTDP-43 (−) MN/AH mean ± SD (%)	ADAR2 (−) pTDP-43 (+) MN/AH mean ± SD (%)	ADAR2 (+) pTDP-43 (+) MN/AH *n* (%)	Number of AH examined
1	67	M	3	1,390	ALS	1 year 1 month	UE	6.0 ± 2.6	1.3 ± 1.5 (20.8)	4.8 ± 2.4 (79.2)	0	4
2	59	F	5	1,290	ALS	1 year 9 months	UE	2.3 ± 1.2	0 ± 0 (0.0)	2.3 ± 0.5 (100)	0	4
3	69	M	3	1,430	ALS	2 years	UE	3.3 ± 1.5	2.3 ± 1.9 (69.6)	1.0 ± 0.8 (30.4)	0	7
4	75	F	2	1,080	ALS	2 years 6 months	LE	8.7 ± 3.1	5.7 ± 2.8 (65.4)	3.0 ± 3.0 (34.6)	1 (0.2)	6
5	72	M	1.5	1,290	ALS	3 years 1 month	Bulb	3.5 ± 1.6	0.5 ± 0.6 (14.3)	3.0 ± 1.2 (85.7)	0	4
6	62	M	3	1,390	ALS	3 years 7 months	UE	4.9 ± 1.7	1.3 ± 0.8 (26.5)	3.6 ± 1.7 (73.5)	0	7
7	69	M	1.5	1,460	ALS	12 years	UMN	2.2 ± 0.7	0.8 ± 0.4 (38.5)	1.3 ± 0.3 (61.5)	0	6
8	64	M	2	1,200	Cerebellar tumor			15.8 ± 8.6	15.8 ± 8.6 (100)	0	0	4
9	58	M	7	1,420	Myotonic dystrophy			13.3 ± 7.2	13.3 ± 7.2 (100)	0	0	4
10	70	F	2	1,040	Limb-girdle muscular dystrophy			10.2 ± 5.4	10.2 ± 5.4 (100)	0	0	6
11	73	M	3	1,170	Theophylline intoxication			8.2 ± 4.9	8.2 ± 4.9 (100)	0	0	6
12	77	M	1.5	1,200	Limb-girdle muscular dystrophy			10.9 ± 6.1	10.9 ± 6.1 (100)	0	0	8
13	78	M	1	1,310	Meningitis			8.4 ± 4.6	8.4 ± 4.6 (100)	0	0	8

PMI postmortem interval, *AH* anterior horn, *MN* motor neuron, *UE* upper extremities, *LE* lower extremities, *Bulb* bulbar symptoms, *UMN* upper motor neuron sign

Double immunofluorescence study using anti-ADAR2 antibody and anti-phosphorylation-independent TDP-43 antibody

Formalin-fixed paraffin-embedded spinal cord sections from an ALS patient (case 6 in Table 1) were double-immunostained with RED1 antibody (×100) and anti-TDP-43 monoclonal antibody (Abnova, ×1,000). Labeled goat anti-rabbit IgG antibody (Molecular Probes, Alexa 488) and labeled goat anti-mouse IgG (Molecular Probes, Alexa 594) were used as secondary antibodies (×1,000).

Quantification of motor neurons in ALS and control spinal cords

Serial sections of both ALS and control cases were immunostained with piTDP-43, ADAR2, or pTDP-43. Large ADAR2-positive and -negative neurons with nucleoli in the anterior horns on each section were counted separately. In addition, we examined whether each of the motor neurons was immunostained with pTDP-43 or piTDP-43 in the respective adjacent section.

Statistics

The Mann–Whitney *U* test was used to compare the number of anterior horn cells (AHC) in ALS samples compared to controls.

Results

Nuclear localization of ADAR2

The Western blot analysis of the human cortex showed that the anti-ADAR2 antibody (RED1) recognized two isoforms of active ADAR2 protein, ADAR2a and ADAR2b, in the nuclear fraction, but not in the cytoplasmic fraction. It is reasonable for ADAR2 to be localized in the nuclear fraction because ADAR2 primarily acts on RNA. The validity of this fractionation was verified by the presence of histone in the nuclear fraction and of GAPDH in the cytoplasmic fraction (Fig. 1a). ADAR2 immunoreactivity is observed in the nuclei of motor neurons from frozen sections of rat (Fig. 1b) and human spinal cords (Fig. 1c).

ADAR2 expression in motor neurons of normal rat and SOD1 transgenic mouse

Intense ADAR2 immunoreactivity was observed in the nucleolus of the nuclei from all motor neurons examined in the frozen rat sections (Fig. 2a, c), whereas both the nucleus and cytoplasm were immunoreactive for ADAR2

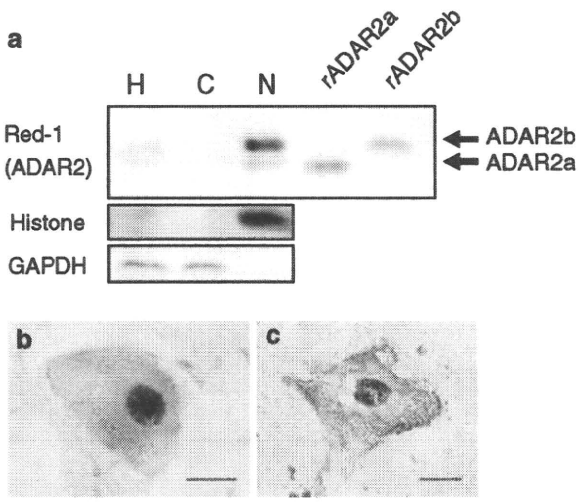

Fig. 1 Nuclear localization of the ADAR2 protein in the human brain. Western blot analysis of the human cortex demonstrates that ADAR2 protein is localized in the nuclear fraction, but not in the cytoplasmic fraction. The validity of this fractionation was verified by the presence of histone in the nuclear fraction and of GAPDH in the cytoplasmic fraction. ADAR2 immunoreactivity is demonstrated in the nuclei of large neurons in the anterior horn of the rat spinal cord (**b**) and the human spinal cord (**c**). *Bar* indicates 20 μm. *N* nuclear fraction, *C* cytoplasmic fraction, *H* brain homogenate, *rADAR2a* recombinant human ADAR2a, *rADAR2b* recombinant human ADAR2b

in the paraffin-embedded sections of both PMI-0 and PMI-6 tissues (Fig. 2b, d, e, g, h). The intensity of ADAR2 immunoreactivity varied markedly among the nuclei (even on the same section) and was uniformly low in the cytoplasm of the motor neurons in the paraffin-embedded sections. ADAR2 immunoreactivity in the nuclei of motor neurons on the frozen and paraffin-embedded sections of PMI-24 tissue was less intense than in PMI-0 and PMI-6 tissues (Fig. 2). ADAR2 immunoreactivity was observed in the nucleus of all the motor neurons examined in the spinal cords of $SOD1^{G93A}$ transgenic mice (Fig. 3b).

ADAR2, phosphorylation-dependent TDP-43 and phosphorylation-independent TDP-43 expression in human control spinal motor neurons

In the spinal cords of human control cases, all motor neurons examined ($n = 380$ from 6 cases) showed ADAR2 immunoreactivity, typically in the cytoplasm with slight or no apparent immunoreactivity observed in the nuclei (Table 1; Figs. 4a, b, 5a). Similar ADAR2 immunoreactivity was observed in all the neurons in the pontine nuclei, including atrophic neurons in patients with multiple system atrophy and spinocerebellar atrophy type 1 (Supplementary Figure 1). Phosphorylation-independent TDP-43 (piTDP-43) stained the nuclei of the same motor